Part I Microalgal biotechnology BPE 35306

Microalgal photosynthesis and growth in mass culture

February 2016

Marcel Janssen

Bioprocess Engineering, Wageningen University and Research

Contents

List of symbols

λ	wavelength	[nm]
α	initial slope q^c_S – I_{ph} curve	$[(mol_S \cdot mol_x^{-1}) \cdot (mol_{ph} \cdot m^{-2})^{-1}]$
μ	specific growth rate	$[s^{-1}]$
μ_m	maximal specific growth rate	$[s^{-1}]$
μ_{PI}	μ calculated from q^c_S – I_{ph} curve	$[s^{-1}]$
$\mu_{PI}(z)$	μ_{PI} at location z in photobioreactor	$[s^{-1}]$
$\overline{\mu}$	average specific growth rate microalgae in photobioreactor	$[s^{-1}]$
$A_{r,light}$	light-exposed surface area of reactor	$[m^2]$
a_x	spectrally-averaged specific light absorption coefficient	$[m^2 \cdot mol_x^{-1}]$
$a_{x,\lambda}$	wavelength-specific light absorption coefficient	$[m^2 \cdot mol_x^{-1}]$
C_x	biomass concentration in photobioreactor system	$[mol_x \cdot m^{-3}]$
$C_{x,opt}$	optimal biomass concentration in photobioreactor (at max r_x)	$[mol_x \cdot m^{-3}]$
d	optical depth of photobioreactor	[m]
D	dilution rate of photobioreactor	$[s^{-1}]$
F	liquid flow rate through photobioreactor	$[m^3 \cdot s^{-1}]$
HRT	hydraulic retention time	[s]
I_{ph}	PAR photon flux density	$[mol_{ph} \cdot m^{-2} \cdot s^{-1}]$
$I_{ph}(z)$	I_{ph} at location z in photobioreactor	$[mol_{ph} \cdot m^{-2} \cdot s^{-1}]$
$I_{ph}(0)$	I_{ph} at location z = 0 (light-exposed surface) in photobioreactor	$[mol_{ph} \cdot m^{-2} \cdot s^{-1}]$
$I_{ph}(d)$	I_{ph} at location z = d (dark surface) in photobioreactor	$[mol_{ph} \cdot m^{-2} \cdot s^{-1}]$
$I_{ph,c}$	compensation photon flux density for photoautotrophic growth	$[mol_{ph} \cdot m^{-2} \cdot s^{-1}]$
$I_{ph,s}$	saturation photon flux density for photosynthesis	$[mol_{ph} \cdot m^{-2} \cdot s^{-1}]$
m_S	specific sugar consumption rate for maintenance	$[mol_S \cdot mol_x^{-1} \cdot s^{-1}]$
q_{ph}	specific photon consumption rate	$[mol_{ph} \cdot mol_x^{-1} \cdot s^{-1}]$
q^c_s	specific sugar (CH_2O) production rate in chloroplast	$[mol_s \cdot mol_x^{-1} \cdot s^{-1}]$
$q^c_{s,m}$	maximal specific sugar (CH_2O) production in the chloroplast	$[mol_s \cdot mol_x^{-1} \cdot s^{-1}]$
$q^c_s(z)$	q^c_s at location z in microalgal culture	$[mol_s \cdot mol_x^{-1} \cdot s^{-1}]$
q_s	specific sugar (CH_2O) consumption rate in microalgal cell	$[mol_s \cdot mol_x^{-1} \cdot s^{-1}]$

r_x	volumetric biomass production rate	[$mol_x \cdot m^{-3} \cdot s^{-1}$]
V_r	Liquid volume of reactor	[m^3]
$Y^c_{s/ph}$	yield of sugar (CH_2O) produced on photons	[$mol_s \cdot mol_{ph}^{-1}$]
$Y^c_{s/ph,m}$	maximal yield of sugar (CH_2O) produced on photons	[$mol_s \cdot mol_{ph}^{-1}$]
$Y_{x/s}$	yield of biomass on sugar (CH_2O)	[$mol_x \cdot mol_s^{-1}$]
$Y_{x/ph}$	yield of biomass on photons	[$mol_x \cdot mol_{ph}^{-1}$]
$Y_{x/ph,m}$	maximal yield of biomass on photons (m_s = 0)	[$mol_x \cdot mol_{ph}^{-1}$]
z	shortest distance to light-exposed surface photobioreactor	[m]
z_s	depth of photobioreactor zone with saturating light, $I_{ph} = I_{ph,s}$	[m]

Subscripts and superscripts

λ	wavelength-specific
c	chloroplast, or compensation
m	maximal
ph	photons
r	reactor
s	sugar (CH_2O), or saturating
x	biomass

Abbreviations

PAR	Photosynthetic Active Radiation, 400 nm to 700 nm
PS	Photosystem

Microalgal photosynthesis and growth in mass culture

Large-scale production of microalgae and cyanobacteria carries a big promise to fill in our future needs for sustainable feedstock for food, feed, chemicals, and possibly fuels. Currently large-scale production is still in its infancy and the few larger production systems in the world are productions plants in the order of a few hectares (ha). A realistic outlook for future scale-up potential is relating microalgae production to greenhouse production of food crops. This comparison is based on the overlap in economics and technology of greenhouse horticulture and that of envisioned large-scale microalgae production. Greenhouse horticulture in The Netherlands, for example, has a total production area of 10 000 ha, and worldwide production is one to two orders of magnitude larger.

In order to facilitate the process of up-scaling a thorough understanding of the microalgal production process is required. This chapter provides a simple methodology to analyze microalgal production systems as related to light exposure. The focus on light is based on the fact that sunlight irradiance will ultimately limit areal productivity and that all other cultivation parameters must be balanced to that number. The close relation to sunlight exposure determines the shape and operation conditions of microalgae productions systems, which will be called photobioreactors. Also pond-based production systems will be considered to be photobioreactors. Other important aspects with respect to photobioreactor design and operation are the adequate supply of carbon dioxide, the removal of oxygen, and temperature control. Gas exchange in bioreactors is well described in numerous engineering books and scientific publications. Temperature control is predominantly limited by technological and environmental limitations.

The light based modelling approach adopted in this chapter is simple allowing for a wide audience while still providing sufficient accuracy and process insight. Despite its simplicity the model is closely linked to the biological understanding of the process of photosynthesis and the fundamental limits of this process. At the end of the chapter the assumptions and simplifications made will be discussed allowing for a reader evaluation which topics must be explored further.

1 Fundamentals of photoautotrophic growth and light

1.1 Photoautotrophic growth

Microalgae grow based on photosynthesis. In Figure 1 this process is schematically introduced. In the chloroplast light energy is absorbed by a large number of photosystems. The photosystems are located on the thylakoid membranes enclosing a space called the lumen. To facilitate light absorption each photosystem (PS) is equipped with an antenna complex composed of a large number of pigment molecules (chlorophylls and carotenoids). Only photons in the wavelength range of 400 to 700 nm are absorbed. This range is called photosynthetic active radiation PAR. When talking about photons in the remainder of this chapter these always reflect PAR photons and the nature of light will be discussed in more detail in the next section. The energy of the absorbed photons is used within the photosystems to transfer electrons from water (H_2O) to oxidized nicotinamide adenine dinucleotide phosphate ($NADP^+$) to yield reduced NADPH and oxygen (O_2). At the same time adenosine triphosphate (ATP) is produced using a proton motive force which is created over the thylakoid membranes. This so-called linear photosynthetic electron transport requires the coordinated action of two types of photosystems, PSII followed by PSI. Two photosystems are needed in order to provide sufficient driving force to move electrons from water to $NADP^+$.

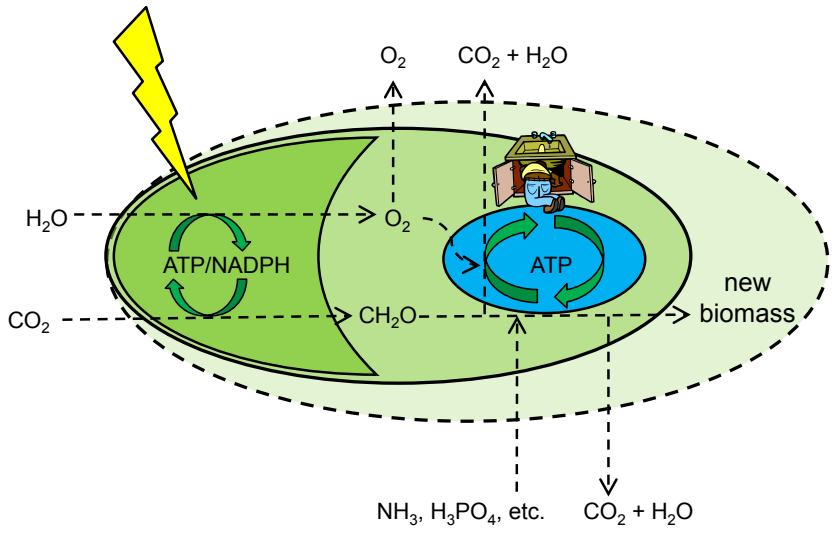

Figure 1: Schematic presentation of photoautotrophic growth of microalgae. The dark green organelle represents the chloroplast where photosynthesis takes place. The blue organelle represents the mitochondria where the respiratory machinery is located. The compound CH_2O represents sugar.

The NADPH and ATP generated is used within the chloroplast to fix carbon dioxide (CO_2) and reduce it to sugar. This sequence of reactions is called the Calvin–Benson–Bassham cycle and this cycle results in the production of the phosphorylated 3-carbon sugar glyceraldehyde 3-phosphate (GAP), also called triose. This triose sugar is exported out of the chloroplast and in this course we will refer to it as CH_2O which is the chemical composition of sugar when normalized to 1 carbon atom.

Sugar (CH_2O) is the building block for new microalgal biomass in the growth reactions. But not all triose ends up in the microalgal biomass. A significant part is broken down and oxidized (respired) in the mitochondria to generate energy in the form of ATP. This ATP is needed to drive, or 'push', the growth reactions, as well as the maintenance reactions. Maintenance is defined as the collection of cellular processes needed to survive not including growth-related processes.

All the sugar (CH_2O) needs to be formed by photosynthesis in the chloroplast. In the Calvin–Benson–Bassham cycle CO_2 is reduced to the level of sugar (CH_2O) according to the following reaction and stoichiometry:

$$CO_2 + 3 \cdot ATP + 2 \cdot NADPH + 2H^+ \rightarrow CH_2O + 3 \cdot ADP + 3 \cdot P_i + 2 \cdot NADP^+ + H_2O$$

The ATP and NADPH required to reduce CO_2 is produced in the light reactions of photosynthesis.

$$2 \cdot H_2O + 2 \cdot NADP^+ + 3 \cdot ADP + 3 \cdot P_i + photons \rightarrow O_2 + 2 \cdot NADPH + 2 \cdot H^+ + 3 \cdot ATP$$

According to this stoichiometry, which is often reported, the amount of ATP and NADPH needed to fix 1 (mol) of CO_2 is equal to the amount which is generated in the light reactions when 2 (mol) H_2O are split generating 1 (mol) O_2. The theoretical minimal amount of light (= photons) needed to generate 2 NADPH and thus 1 O_2 is 8 photons. This number is based on the functioning of linear photosynthetic electron transport requiring the coordinated action of two type of photosystems (PSII and PSI) to extract 4 electrons from two water molecules leading to two molecules of NADPH.

In the stoichiometry of the light reactions above it is implicitly assumed that 8 protons (H^+) are transported over the thylakoid membranes during linear electron transport assuming a fully functional Q-cycle (Cape et al. 2006). Together with the 4 protons (H^+) released when oxidizing water the lumen is thus enriched with 12 H^+. It is assumed that these 12 H^+ drive the production of 3 ATP in the thylakoid ATP-ase enzyme complex. The real stoichiometry between protons (H^+) trans-located and ATP produced by the ATP-ase enzyme complex of microalgae probably is different from this 12:3 (H^+:ATP) ratio. For spinach chloroplasts the ratio was determined to be 14:3 (Vollmar et al. 2009; Seelert et al. 2000), and also for *Chlamydomonas* and cyanobacteria ratios of 13:3, 14:3 and 15:3

have been reported (Meyer Zu Tittingdorf et al. 2004; Pogoryelov et al. 2007). This results in less ATP produced then required in the Calvin–Benson cycle since we cannot allow for the accumulation of reduced NADPH. The resulting lack of ATP then is suggested to be compensated by cyclic photosynthetic electron transport around photosystem I (PSI) yielding only ATP (Allen 2003) by generating a proton motive force across the thylakoid membrane. Cyclic electron transport driven by PSI allows for the transport of 2 protons (H+) over the thylakoid membranes per photon absorbed. Consequently, minimally 9 photons are used to reduce one CO_2 to the level of sugar.

$$2 \cdot H_2O + 2 \cdot NADP^+ + 3 \cdot ADP + 3 \cdot P_i + 9 \cdot h\nu \rightarrow O_2 + 2 \cdot NADPH + 2 \cdot H^+ + 3 \cdot ATP$$

By combining the Calvin–Benson–Bassham cycle with the light reactions the following general reaction of photosynthesis is then obtained.

$$CO_2 + H_2O + 9 \cdot h\nu \rightarrow CH_2O + O_2$$

Under optimal conditions in the laboratory at low photon flux density a photon requirement (or quantum requirement) of 9 for O_2 production or CO_2 fixation, however, is rarely measured. The most realistic assumption of the minimal quantum requirement seems to be a value of 10. This is based on an analysis of dedicated research in this field: Oxygen exchange measurements with leaf–disc electrodes for higher plants (Evans 1987; Björkman & Demmig 1987); laser-induced oxygen flash yield measurements (Ley & Mauzerall 1982; Dubinsky et al. 1986); photoacoustic and photothermal calorimetry, as reflected upon by (Malkin & Fork 1996).

A quantum requirement of 10 thus means that the maximal yield of sugar (CH_2O) on photons is equal to 0.10. This number will be called the maximal yield of sugar on photons $Y^c_{s/ph,m}$ with unit $mol_S \cdot mol_{ph}^{-1}$. This parameter will be very important later when describing photoautotrophic growth in a mathematical model.

In Figure 2 the most important production and consumption rates in photoautotrophic growth are presented. Here '*q*' rates are used which represent biomass specific production and consumption rates with unit $mol \cdot mol_x^{-1} \cdot s^{-1}$ (symbol 'x' reflects biomass). Later when moving from a cellular approach to a reactor approach volumetric production and consumption rates will be introduced designated with symbol '*r*' and unit $mol \cdot m^{-3} \cdot s^{-1}$. Volumetric rates are the products of specific rates '*q*' and the concentration of biomass in the bioreactor C_x.

Based on the reaction stoichiometry the following can be said about the corresponding specific consumption and production rates in the chloroplast:

$$-q^c_{CO2} = -q^c_{H2O} = q^c_s = q^c_{O2} \qquad [\text{mol}\cdot\text{s}^{-1}]$$

The specific rate of sugar production in the chloroplast q^c_s thus is a direct measure of the rate of photosynthesis and is equivalent to the specific rate of oxygen (O_2) production or carbon dioxide (CO_2) fixation, which are also used as measures of photosynthesis. The superscript 'c' is used to denote that these reactions take place in the chloroplast.

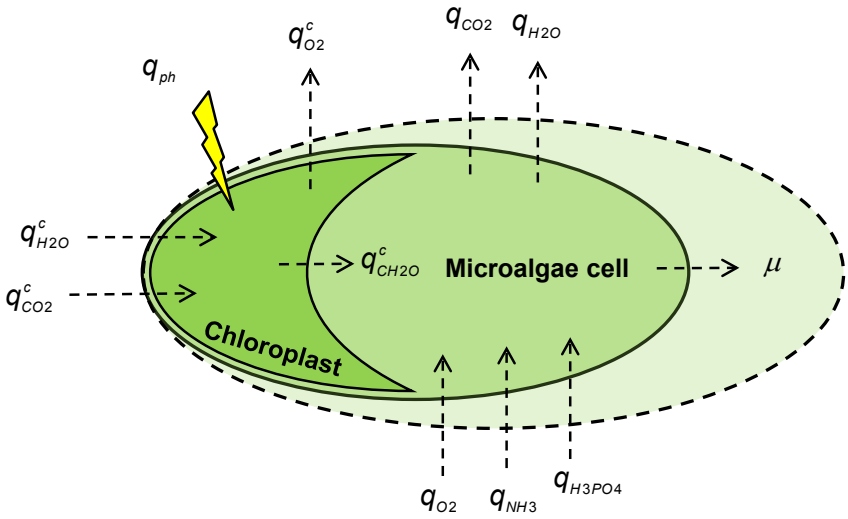

Figure 2: Representation of most important specific consumption and production rates for the quantitative analysis of photoautotrophic growth. The superscript '*c*' reflects the chloroplast

The sugar (CH_2O) produced In the chloroplast is the building block of real biomass. Below a generalized reaction is shown without any stoichiometry where the compound $CH_{xH}O_{xO}N_{xN}P_{xP}$ represents biomass. So, 1 mol of this compound $CH_{xH}O_{xO}N_{xN}P_{xP}$ will be called 1 mol_x. All other elements present in biomass (S, K, Mg, Ca, Fe, and others) because they do not contribute a lot on a mass basis.

$$CH_2O + O_2 + NH_3 + H_3PO_4 \rightarrow CH_{xH}O_{xO}N_{xN}P_{xP} + CO_2 + H_2O$$

Not all sugar CH_2O produced by photosynthesis ends up in the biomass. A considerable part of the sugar (CH_2O) needs to be broken down and oxidized to provide energy (ATP) to support the growth reactions. In addition, additional energy (ATP) is needed for maintenance. Maintenance refers to the collection of cellular processes needed to survive not including growth related processes.

The growth-related sugar consumption is a very important aspect for an accurate quantitative description of microalgal growth. In the mitochondria of microalgae part of the triose sugar is thus degraded in the citric acid cycle and the generated reductant is oxidized (i.e. oxidative

phosphorylation) generating considerable ATP necessary to drive all growth reactions. In several published analyses of microalgal growth a constant respiration is assumed. In reality respiration is thus coupled to growth, and this has been well-documented (Kliphuis, Janssen, et al. 2011; Geider & Osborne 1989). In fact, the chloroplast can be seen as a sugar factory. Accordingly, considering the general process occurring outside of the chloroplast this process can be well described by aerobic chemoheterotrophic growth.

A simple substrate balance according to Pirt (Pirt 1965) can be used to couple the specific consumption rate of sugar outside of the chloroplast q_s to the specific growth rate μ of the microalgae.

$$q_s = -\frac{\mu}{Y_{x/s}} - m_s$$

Please note that this specific sugar consumption rate q_s is equal to the specific sugar production rate in the chloroplast q^c_s but of opposite sign. The parameter μ represent the specific growth rate of the microalgae and has unit s^{-1}. The parameter m_s is the specific sugar consumption rate to provide energy (ATP) for maintenance with unit $mol_s \cdot mol_x^{-1} \cdot s^{-1}$. Its value is difficult to measure and also depends on the microalgal species and growth conditions (for example temperature). Typical values for microalgae found in the laboratory are in the range of $1 \cdot 10^{-6}$ to $5 \cdot 10^{-6}$ $mol_s \cdot mol_x^{-1} \cdot s^{-1}$.

The parameter $Y_{x/S}$ represents the yield of microalgal biomass on sugar with units $mol_x \cdot mol_s^{-1}$. Studies under heterotrophic and mixotrophic conditions with glucose as a carbon source show a maximal yield of about 0.5 $g \cdot g^{-1}$ translating in 0.625 $mol_x \cdot mol_s^{-1}$ (Li et al. 2014; Shi et al. 1997; Chen & Johns 1991; Lee et al. 1996). It has to be stressed that these numbers reflect nutrient replete growth with 'normal' protein content. Biomass accumulating starch will result in somewhat higher yields. Microalgae accumulating lipids probably will result in somewhat lower yields. In this chapter we will not discuss such product accumulation and we will only consider nutrient replete growth. Also the nitrogen source will affect the biomass yield on sugar since nitrate is much more oxidized than ammonia or urea. The higher yields of 0.625 $mol_x \cdot mol_s^{-1}$ are usually reported with ammonium and urea as a nitrogen source. For example, a recalculation of the data of Kliphuis result in a biomass yield of 0.52 $mol_x \cdot mol_s^{-1}$ for growth on nitrate of the green microalga *Chlamydomonas*.

The separation of photosynthetic sugar production in the chloroplast from actual microalgal biomass production from triose sugars allows for a comparison with aerobic chemoheterotrophic growth. The maximal biomass yield on sugar for aerobic chemoheterotrophic growth (bacteria and yeasts) is

reported to range between 0.4 and 0.7 $mol_x \cdot mol_s^{-1}$, and it is bound by thermodynamic constraints (Heijnen & Van Dijken 1992; Heijnen 1994; von Stockar & Liu 1999). Based on this comparison with yeast and bacteria, it will be assumed that the microalgal biomass yield on photosynthetically derived sugar probably will be somewhere between 0.5 and 0.65 $mol_x \cdot mol_s^{-1}$, and that it will definitely not be higher than 0.7 $mol_x \cdot mol_s^{-1}$.

The analysis of microalgal growth presented in this chapter in principle could be extended to include growth of photoautotrophic cyanobacteria. Cyanobacteria do not have separate organelles for photosynthesis and respiration (i.e. chloroplasts and mitochondria). The photosynthetic and respiratory chains are located on the same thylakoid membranes which form stacks of parallel sheets close to the cytoplasmic membrane. The photosynthetic and respiratory electron transport chains share a number of components leading to alternative electron transport routes (Mullineaux 2014; Vermaas 2001). Without going into detail in the light cyanobacteria can generate additional ATP via either increased cyclic photosynthetic electron transport around PSI, or re-directing reducing equivalents generated by PSII to respiratory components on the thylakoids (Mullineaux 2014). Similar to microalgae this additional ATP is required to support the growth reactions.

The amount of ATP required to support growth starting form sugar will be comparable between cyanobacteria, microalgae, and other aerobic micro-organisms, with a similar macromolecular composition. But one could ask the question what is the most efficient way to produce ATP considering light as a limiting substrate. Cyclic electron transport around PSI seems a simple process but it requires 2.35 photons to generate 1 ATP (Allen 2003). An analysis of Kliphuis (Kliphuis et al. 2012) showed that photosynthetic production of triose sugar in the chloroplast, followed by its breakdown in the mitochondria, requires 1.5 photons to generate 1 ATP. Of course the latter pathway involves more components (proteins) representing a bigger burden for the cell. Only complex metabolic modelling including the costs of the biosynthetic machinery required will allow for the identification of the most efficient pathways (Kramer & Evans 2011; Nogales et al. 2012). At this stage it is important to note there is no proof that either microalgae or cyanobacteria are more efficient in employing light for biomass growth.

Under short periods of darkness also cyanobacteria will rely on the breakdown of sugar-based metabolites to generate reductant to generate ATP via oxidative phosphorylation. Under long periods

of darkness both microalgae and cyanobacteria mobilize sugar form starch or glycogen reserves to support growth and maintenance processes.

To summarize already three important constants necessary for a quantitative model description of microalgal growth have been introduced:

- $Y^c_{s/ph,m}$ - maximal yield of sugar (CH_2O) on photons in the chloroplast [$mol_s \cdot mol_{ph}^{-1}$].
- $Y_{x/s}$ - yield of biomass on sugar (CH_2O) [$mol_x \cdot mol_s^{-1}$]
- m_s - specific sugar consumption rate for maintenance [$mol_s \cdot mol_x^{-1} \cdot s^{-1}$]

In addition, two important variables have been introduced which will appear in a growth model:

- q^c_s - specific sugar (CH_2O) production rate in chloroplast [$mol_s \cdot mol_x^{-1} \cdot s^{-1}$]
- μ - specific growth rate of microalgae [$mol_x \cdot mol_x^{-1} \cdot s^{-1} = s^{-1}$]

Please not that: $q^c_s = -q_s$, with q_s the specific sugar consumption rate of the microalgae.

1.2 Light and photosynthesis

In a scientific context light is electromagnetic radiation of any wavelength. On the other hand, it is also defined as that part of the electromagnetic spectrum which can be sensed by the human eye. For this part of the spectrum, located between 400 and 700 nm, it is therefore best to talk about visible light. In Figure 3 the relative sensitivity of the human eye to visible light of different wavelengths is presented. It is clear that we are most sensitive for green light (555 nm).

Microalgae absorb and use light from the whole visible wavelength range, 400 to 700 nm. But, as will be shown later, the sensitivity of microalgae for visible light of a specific wavelength differs dramatically from our sensitivity. This is also the reason why the lumen, the unit for the luminous flux, cannot, and should not, be used in photosynthesis. The lumen, derived from the candela (the base SI unit), is weighed by the sensitivity of the human eye (Figure 3). For this reason, always radiometric units must be used in photosynthesis instead of photometric units. The radiometric analogue of the lumen (luminous flux) is the watt (radiant flux). At each wavelength both are coupled according to the standard observer curve: At 555 nm one watt of radiant flux corresponds to a luminous flux of 683 lumens by definition. As a comparison, at 650 nm, 1 watt corresponds to 73 lumens only.

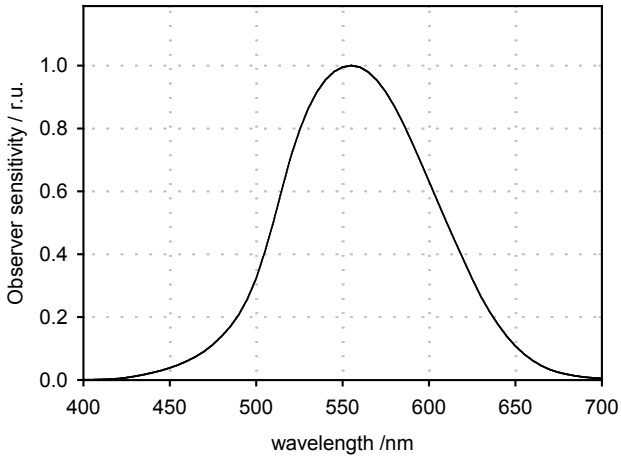

Figure 3: CIE 1931 Standard Colorimetric Observer curve. CIE: Commission Internationale de l'Eclairage

Photosynthesis is a quantum process. The actual absorption of quanta or photons by the microalgal photosystems sets in motion the cascade of reactions ultimately resulting in growth. As such, the radiant flux in Watts, W (= $J \cdot s^{-1}$), is usually converted into a photon flux in $mol_{ph} \cdot s^{-1}$ employing the Planck-Einstein relation ($E = h \cdot \nu$). Light meters used in photosynthesis research are adapted to immediately give the photon flux density in $mol_{ph} \cdot m^{-2} \cdot s^{-1}$ within the PAR wavelength range of 400 to 700 nm. Please note that in this chapter the symbol I_{ph} is used for the photon flux density in the PAR range and that the photon flux density I_{ph} sometimes is referred to by the term 'light intensity'.

In Figure 4 the spectral response of a typical light meter used in photosynthesis research is demonstrated. Using specific filters the meter is made equally sensitive for any photon within the range of photosynthetically active radiation (PAR) which corresponds to the 400-700 nm range.

Microalgae, and all other photosynthetic organisms, need light energy (photons) to grow. Outdoors it is the sun supplying all light energy. On the other hand, also artificial light can be used to grow algae. For the production of very high-value compounds microalgal cultivation on artificial light can be an attractive alternative. But, even when taking into account the continual development of LED lighting in combination with very efficient photosynthesis the combined costs for investment in lamps and consumed power will add about 16 $ of production costs per kg of dry biomass produced (Blanken et al. 2013). The impact of employing artificial light for microalgae production is not only a cost factor but also includes an energy factor. Converting electricity to light (photons) leads to large energy losses

(65% or more) depending on the light source used. Moreover, all electricity needed must be generated.

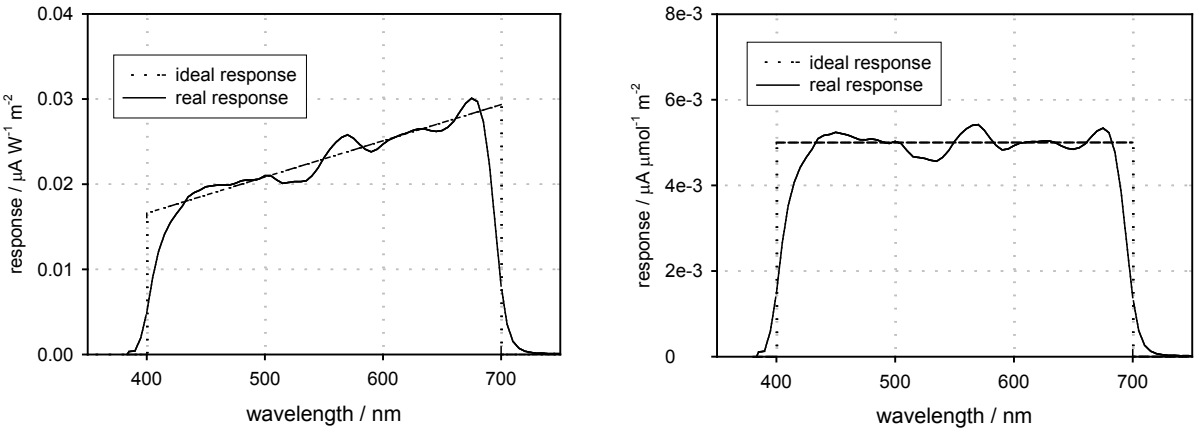

Figure 4: Sensitivity of a LI-190SA quantum sensor (LI-COR Biosciences, Lincoln, NE, USA) for Photosynthetically Active Radiation (PAR). The graph was redrawn from the datasheet delivered with the sensor.

A wide variety of lamps exist and the spectral distribution of a number of lamps used in microalgae research are shown in Figure 5. Only the distribution within the PAR range is shown and all spectra are normalized such that the integral photon flux density over the PAR range is unity. The spectral distribution of sunlight is shown in Figure 6. Between 42 and 43 % of the sun's radiant flux reaching Earth's surface falls within the PAR between 400 and 700 nm. Comparing the spectra of all these different lamps with those of the sun it is evident that all are different from the sun. That should not be a problem because photosynthesis can be fueled with any photon within the PAR range although certain spectral effects cannot be excluded. Timing of cell division, for example, has been shown to depend on light color (Oldenhof et al. 2006).

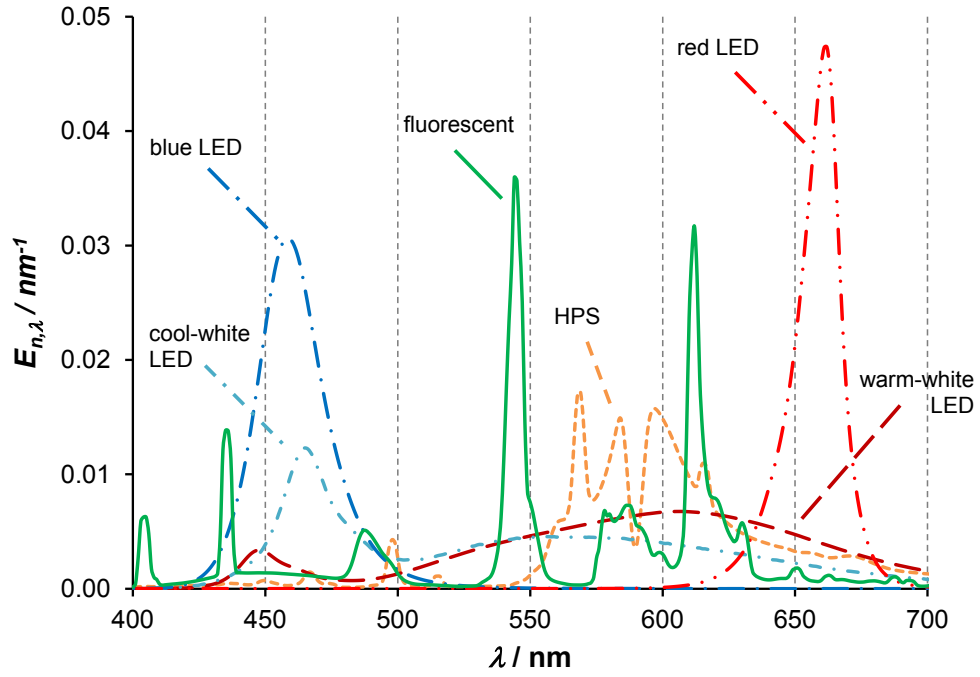

Figure 5: Spectral distribution of artificial lamps employed in microalgae research sunlight at ground level. The spectra are normalized to PAR light, $E_{n,\lambda}$ with units nm^{-1} (i.e. the area under all curves is unity). The tungsten-halogen lamps were placed behind a 1 cm water filter.

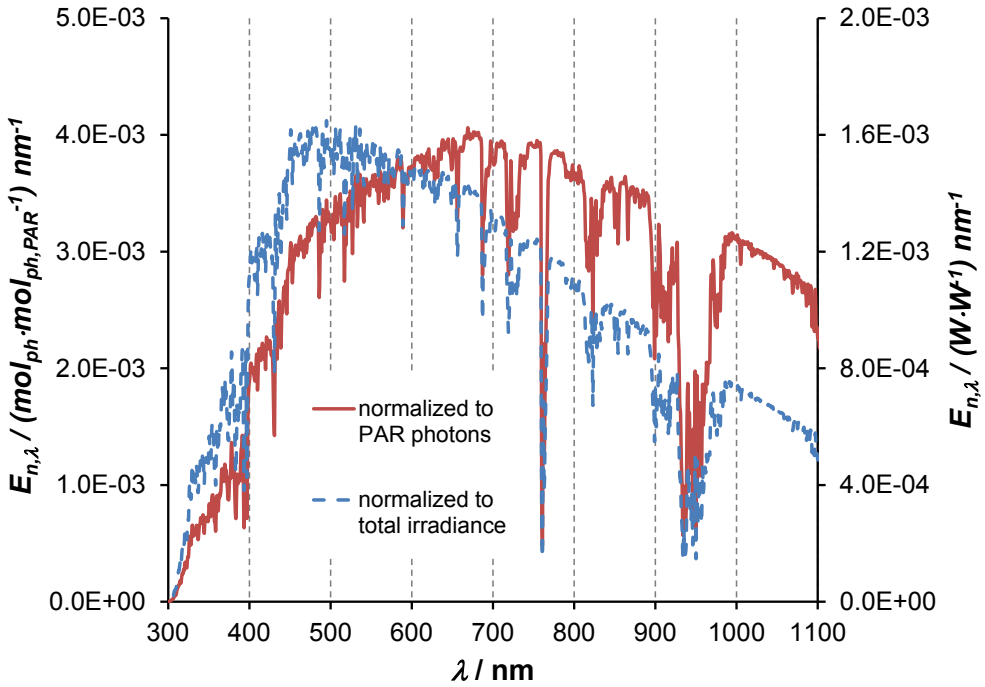

Figure 6: Spectral distribution of sunlight at ground level (ASTM G173-03). The spectrum is normalized to PAR light as well as total irradiance

Irradiance from the sun depends on the geographic position, the season, and the hour. As an example the average hourly irradiance in the month of July in Athens (Greece) and Amsterdam (Netherlands) is presented in Figure 7. The maximal irradiance in Athens is 860 $W \cdot m^{-2}$, which corresponds to more than $1.65 \cdot 10^{-3}$ $mol_{ph} \cdot m^{-2} \cdot s^{-1}$ in the PAR range (400-700 nm). As will be explained later this is a very high light intensity and it is more than sufficient to saturate photosynthesis. At higher latitudes such as Amsterdam the average irradiance is less as can be seen in Figure 7. In July average peak irradiance is 516 $W \cdot m^{-2}$, corresponding to $1.00 \cdot 10^{-3}$ $mol_{ph} \cdot m^{-2} \cdot s^{-1}$ of PAR. This value is lower than the irradiance in Athens predominantly because of increased cloud cover. Also in Amsterdam on a clear-sky day the photon flux density will increase to values of $1.50 \cdot 10^{-3}$ $mol_{ph} \cdot m^{-2} \cdot s^{-1}$ around solar noon.

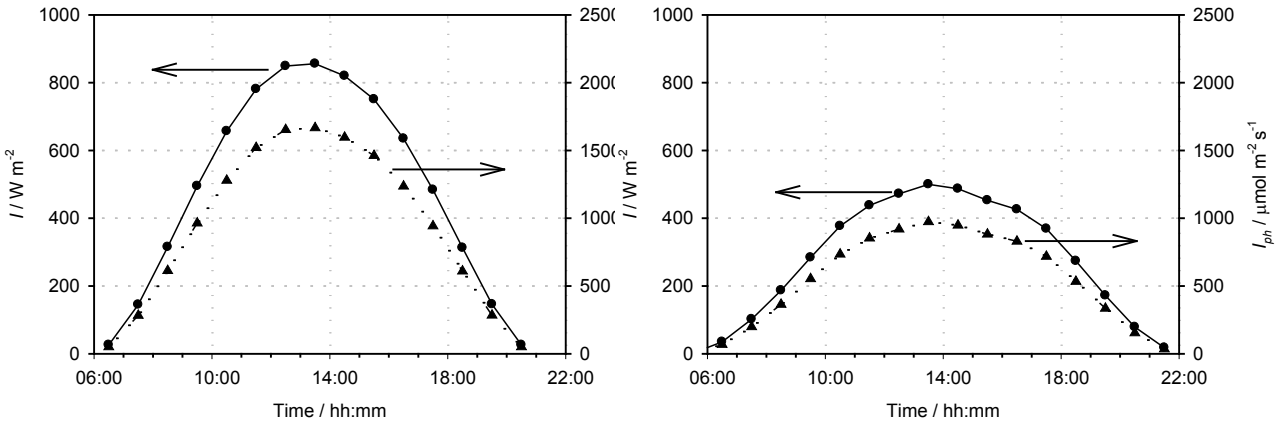

Figure 7: Average Irradiance I and photon flux density I_{ph} on a horizontal surface in Athens (a), Greece, Lat: 37°58'N, and Amsterdam (b), the Netherlands, Lat: 52°21'N, in the month of July. Data are based on values collected from 1996 – 2000 made available by S@tel-Light (The European database of daylight and solar radiation).

As can be seen in Figure 5 and Figure 6 the light emission of artificial lamps and sunlight varies over the PAR wavelength range (400-700 nm). Using PAR quantum sensors we do not see how light is distributed over the PAR wavelength range. As will be discussed elsewhere in this chapter microalgal light absorption also varies over the PAR wavelength range. This implies that when calculating light absorption we have to take this distribution into account and for this reason we will distinguish between the photon flux density I_{ph} and the wavelength-dependent photon flux density $I_{ph,\lambda}$. The I_{ph} is the total photon flux density in the PAR range expressed in $mol_{ph} \cdot m^{-2} \cdot s^{-1}$. $I_{ph,\lambda}$, on the other hand, gives the photon flux density at wavelength λ in a 1 nm interval and consequently has units $mol_{ph} \cdot m^{-2} \cdot s^{-1} \cdot nm^{-1}$.

The I_{ph} can be calculated from $I_{ph,\lambda}$ by integrating $I_{ph,\lambda}$ over the PAR range according to:

$$I_{ph} = \int_{400}^{700} I_{ph,\lambda} \cdot d\lambda \qquad [\text{mol}_{ph} \cdot \text{m}^{-2} \cdot \text{s}^{-1}]$$

This integral is equivalent to the area under the curve in Figure 8 between 400 and 700 nm. The integral suggest that $I_{ph,\lambda}$ can be accurately described by a mathematical equation. In reality this is not always evident and this 'integral' therefore is commonly solved numerically based on the measured $I_{ph,\lambda}$ over small wavelength intervals ($\Delta\lambda$), preferably as small as 1 nm. Mathematically this can be described by using the summation symbol Σ according to:

$$I_{ph} = \sum_{\lambda=400}^{\lambda=700} I_{ph,\lambda} \cdot \Delta\lambda \qquad [\text{mol}_{ph} \cdot \text{m}^{-2} \cdot \text{s}^{-1}]$$

Based on I_{ph} and $I_{ph,\lambda}$ we can now define a normalized spectral distribution of the PAR photons, $E_{n,\lambda}$, according to:

$$E_{n,\lambda} = \frac{I_{ph,\lambda}}{I_{ph}} \qquad [\text{nm}^{-1}]$$

The parameter $E_{n,\lambda}$ has units nm^{-1} and it gives the fraction of PAR photons present in a 1-nm wavelength interval. Sunlight has its own characteristic distribution $E_{n,\lambda}$, just like any artificial light source, and the parameter $E_{n,\lambda}$ is very useful in calculations as will be shown elsewhere in this chapter and this parameter was also used in to Figure 8 illustrate the spectral distribution of different light sources.

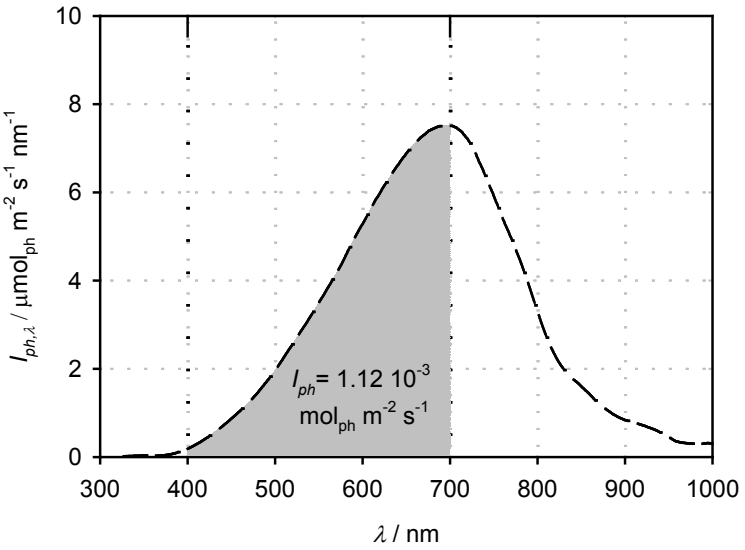

Figure 8: Wavelength-dependent photon flux density ($I_{ph,\lambda}$ in $\mu\text{mol}_{ph} \cdot \text{m}^{-2} \cdot \text{s}^{-1} \cdot \text{nm}^{-1}$) measured inside a bench-scale photobioreactor illuminated with tungsten-halogen lamps. The lamps were placed behind a 1 cm water filter. The photon flux density over whole the PAR range (I_{ph} in $\text{mol}_{ph} \cdot \text{m}^{-2} \cdot \text{s}^{-1}$) is also given and is equivalent to the area below the $I_{ph,\lambda}$–curve between 400 and 700 nm.

2 Quantifying light-limited microalgal growth

2.1 Light absorption

Light is absorbed by the pigments in the antennae of the photosystems, which are located on the thylakoid membranes in the chloroplast. The amount of pigments and their packing determines which fraction of the light falling on a microalgal cell will be absorbed. This fraction can be directly calculated from the specific light absorption coefficient which is also called the optical cross section of microalgae.

When a light beam hits a microalgal cell a fraction of the light is absorbed by the pigments, number 1 in Figure 9. A large fraction of the light, however, will simply pass through the cells unabsorbed. This fraction usually is refracted over a small angle due to the difference of the indices of refraction of the different cellular compartments/structures with the index of refraction of the surrounding water, beam number 3 in Figure 9. Light can also be reflected right at the cellular surface and change direction, number 2 in Figure 9. The reflected and refracted light is still available for other microalgal cells and is not lost. The sum of reflection and refraction is called scattering. Besides using geometrical optics scattering can also be explained and described based on electromagnetic theory employing the MIE theory (Kirk 1994).

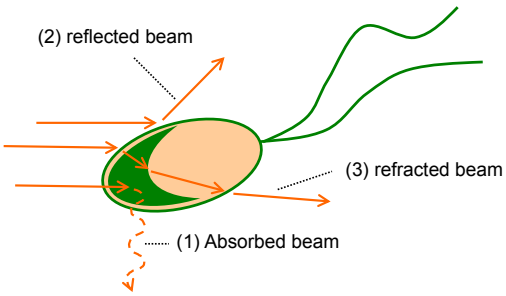

Figure 9: Light absorption and scattering by microalgal cells. Scattering is the sum of reflection and refraction events of light rays by the (sub)cellular structures with different indices of refraction than that of the surrounding water.

In general scattering occurs over small angles depending on the size and shape of the microalgal cells as well as their intracellular composition and compartmentalization (Kirk 1994). In the remainder of this chapter we will neglect the influence of scattering and assume that light is either absorbed, or passes through the cell without changing direction. At the end of the chapter the impact of this assumption will be qualitatively addressed. Light absorption by microalgal cells can be calculated based on the size of the light absorbing surface perpendicular to the light beam/rays. This optical cross section of the cell is also called the specific light absorption coefficient, $a_{x,\lambda}$ (figure 16). This coefficient will be different for

light of different wavelength and it depends on the actual pigment composition of the microalgal cells. For green microalgae, for example, the optical cross section for green light is much smaller than for blue light and red light, see Figure 10. The optical cross section can only be measured in specialized spectrophotometers which only measure light absorption and thus correct for the effect of light scattering (Merzlyak & Razi Naqvi 2000; Davies-Colley et al. 1986).

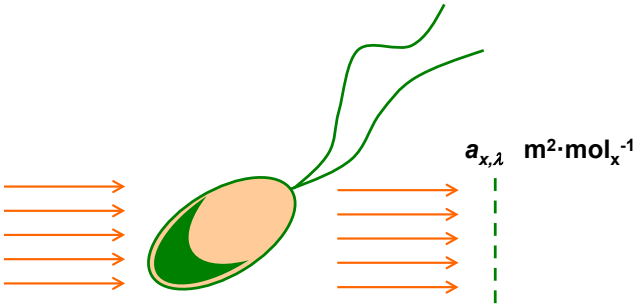

Figure 10: Optical cross section of microalgal cells: the specific absorption coefficient $a_{x,\lambda}$.

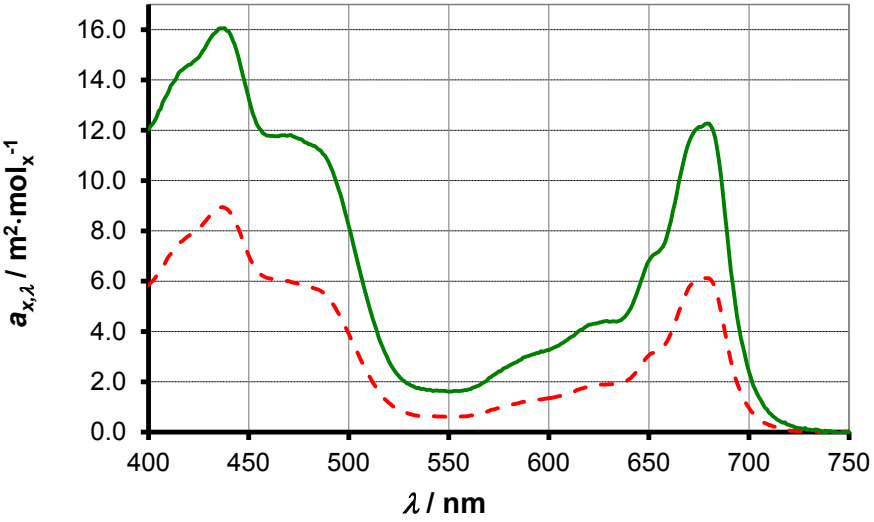

Figure 11: The specific light absorption coefficient $a_{x,\lambda}$ of green microalgae as a function of the wavelength λ. The example given is based on *Chlorella sorokiniana*. The solid green line is a typical example of low-light acclimated microalgae. The dashed red line is a typical example of high-light acclimated microalgae.

Microalgae will acclimate to the light regime they experience. In case the algae are light limited they will respond by increasing their pigmentation and, as such, their specific absorption coefficient $a_{x,\lambda}$. This process is called photoacclimation (Dubinsky & Stambler 2009). High-light acclimated cells have smaller absorption coefficient than low-light acclimated cells and this is illustrated in Figure 11. Results

of the laboratory of Bioprocess Engineering (Wageningen University, The Netherlands) with microalgae of the species *Chlorella*, *Chlamydomonas*, *Scenedesmus*, *Neochloris*, and *Nannochloropis*, show that the under nutrient replete conditions low-light acclimated microalgae express a specific absorption coefficient which is not more than two times larger than those of high-light acclimated microalgae.

The specific light absorption coefficient is a crucial parameter when analysing microalgae production processes. Later it will be discussed how this parameter can be used to estimate light penetration in microalgal cultures inside photobioreactors while neglecting the effect of light scattering. Here it will first be explained that this parameter can also be used to calculate the specific photon absorption rate q_{ph} of microalgae.

When taking into account the spectral distribution of light the specific photon absorption rate q_{ph} can be calculated as follows:

$$-q_{ph} = \sum_{\lambda=400}^{\lambda=700} a_{x,\lambda} \cdot I_{ph,\lambda} \cdot \Delta\lambda \qquad [\mathrm{mol_{ph} \cdot mol_x^{-1} \cdot s^{-1}}]$$

Please note that a minus '-' sign is added to q_{ph} because its real value should be negative since it represents a consumption term. This expression can be simplified by assuming a constant specific light absorption coefficient over the PAR range a_x:

$$-q_{ph} = a_x \cdot I_{ph} \qquad [\mathrm{mol_{ph} \cdot mol_x^{-1} \cdot s^{-1}}]$$

Both relations above are in agreement when a_x is defined as follows:

$$a_x = \sum_{\lambda=400}^{\lambda=700} a_{x,\lambda} \cdot E_{n,\lambda} \cdot \Delta\lambda \qquad [\mathrm{m^2 \cdot mol_x^{-1}}]$$

$$E_{n,\lambda} = \frac{I_{ph,\lambda}}{I_{ph}} \qquad [\mathrm{nm^{-1}}]$$

In other words, the parameter a_x is a spectrally-averaged specific absorption coefficient. Typical values for a_x for green microalgae averaged for sunlight are:

Low-light acclimated cells: $a_x \approx 5-7$ $[\mathrm{m^2 \cdot mol_x^{-1}}]$

High-light acclimated cells: $a_x \approx 2.5-3.5$ $[\mathrm{m^2 \cdot mol_x^{-1}}]$

2.2 Photosynthesis

In well-designed photobioreactors light is usually the growth limiting 'substrate'. So, how does microalgal growth depend on light? First models will be introduced describing photosynthetic sugar production rate in the chloroplast as a function of photon flux density. The triose sugar produced in the chloroplast is consumed again in the rest of the cell. From the specific sugar consumption rate the specific growth rate of the microalgae can be calculated as explained hereafter.

The specific sugar production rate in the chloroplast q^c_s thus depends on the photon flux density I_{ph}. This relation can be described by the following model based on the hyperbolic tangent function, the model of Jassby & Platt (Jassby & Platt 1976).

$$q^c_s = q^c_{s,m} \cdot \tanh\left(\frac{\alpha \cdot I_{ph}}{q^c_{s,m}}\right) \qquad [\mathrm{mol_s \cdot mol_x^{-1} \cdot s^{-1}}]$$

Sugar is defined as the 1-carbon equivalent of any sugar molecule (e.g. triose or hexose) thus having elemental composition CH_2O.

The hyperbolic tangent function is composed of exponential components and can also be written differently:

$$\tanh x = \frac{\sinh x}{\cosh x} = \frac{e^x - e^{-x}}{e^x + e^{-x}} = \frac{e^{2x} - 1}{e^{2x} + 1}$$

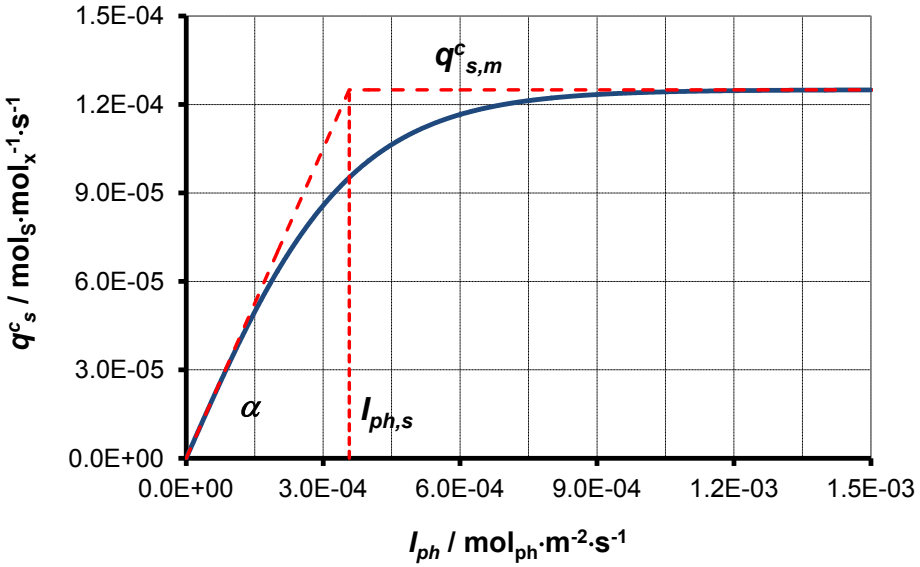

Figure 12: The specific rate of photosynthesis as a function of photon flux density I_{ph} according to the model of Jassby & Platt. Photosynthesis is represented by the specific sugar production rate in the chloroplast q^c_s. Parameter values based on high-light acclimated *Chlorella sorokiniana*: a_x = 3.5 $m^2 \cdot mol_x^{-1}$; $Y^c_{s/ph,m}$ = 0.10 $mol_s \cdot mol_{ph}^{-1}$; $q^c_{s,m}$ = $1.25 \cdot 10^{-4}$ $mol_s \cdot mol_x^{-1} \cdot s^{-1}$; M_x = 24 $g \cdot mol_x^{-1}$.

This relation between the specific rate of photosynthesis and photon flux density is shown in Figure 12. The term photosynthesis thus reflects only sugar production in the chloroplast and not biomass growth as a whole which will be covered hereafter. The specific rate of photosynthesis first increases rapidly with increasing photon flux density. At higher photon flux density the increase slows down and eventually the rate of photosynthesis reaches a maximum. As can be seen in Figure 12 the specific rate of photosynthesis q^c_s will approach $q^c_{s,m}$ at high photon flux density. The parameter $q^c_{s,m}$ thus represents the maximal photosynthetic capacity of the cell and it depends on microalgal species as well as cultivation temperature. The parameter α represents the initial slope of the curve when the photons flux density equals 0 $mol_{ph} \cdot m^{-2} \cdot s^{-1}$.

The parameter α also carries a biological meaning. It can be described as the product of the maximal yield of sugar on photons (in the chloroplast), $Y^c_{s/ph,m}$, and the spectrally averaged absorption coefficient a_x.

$$\alpha = Y^c_{s/ph,m} \cdot a_x$$

A good estimate of $Y^c_{s/ph,m}$ is 0.10 and this was already discussed before. The parameter α can thus be replaced with the product of two parameters with a biological meaning and then the following expression is obtained:

$$q^c_s = q^c_{s,m} \cdot \tanh\left(\frac{Y^c_{s/ph,m} \cdot a_x \cdot I_{ph,}}{q^c_{s,m}}\right) \qquad [mol_s \cdot mol_x^{-1} \cdot s^{-1}]$$

The parameter a_x can also be combined (i.e. multiplied) with variable I_{ph} giving the specific photon absorption rate. Please note that the following relation for the specific rate of photon absorption was already introduced:

$$-q_{ph} = a_x \cdot I_{ph} \qquad [mol_{ph} \cdot mol_x^{-1} \cdot s^{-1}]$$

And thus also the following relation for the specific rate of sugar production can be obtained:

$$q^c_s = q^c_{s,m} \cdot \tanh\left(\frac{Y^c_{s/ph,m} \cdot -q_{ph}}{q^c_{s,m}}\right) \qquad [mol_s \cdot mol_x^{-1} \cdot s^{-1}]$$

The last form is particularly useful when calculating photobioreactor productivity as will be discussed later.

For the sake of simplicity an alternative model will be introduced which will prove to be very useful when analysing photobioreactor productivity. This one is based on Blackman kinetics (Blackman 1905) and it follows the dashed lines in Figure 12. According to this model the rate of photosynthesis

increases linearly with increasing photon flux density with the proportionality constant being α. When a saturating photon flux density of $I_{ph,s}$ is reached photosynthesis reaches its maximal level and remains constant at $q^c_{s,m}$.

Mathematically this model is described as follows:

$$I_{ph} \le I_{ph,s} \qquad q^c_s = \alpha \cdot I_{ph}$$

$$I_{ph} \ge I_{ph,s} \qquad q^c_s = q^c_{s,m}$$

As explained before the parameter α carries a biological meaning and it can be described as follows:

$$\alpha = Y^c_{s/ph,m} \cdot a_x$$

So, the saturating photon flux density $I_{ph,s}$ can be calculated as follows:

$$I_{ph,s} = \frac{q^c_{s,m}}{\alpha} = \frac{q^c_{s,m}}{a_x \cdot Y^c_{s/ph,m}}$$

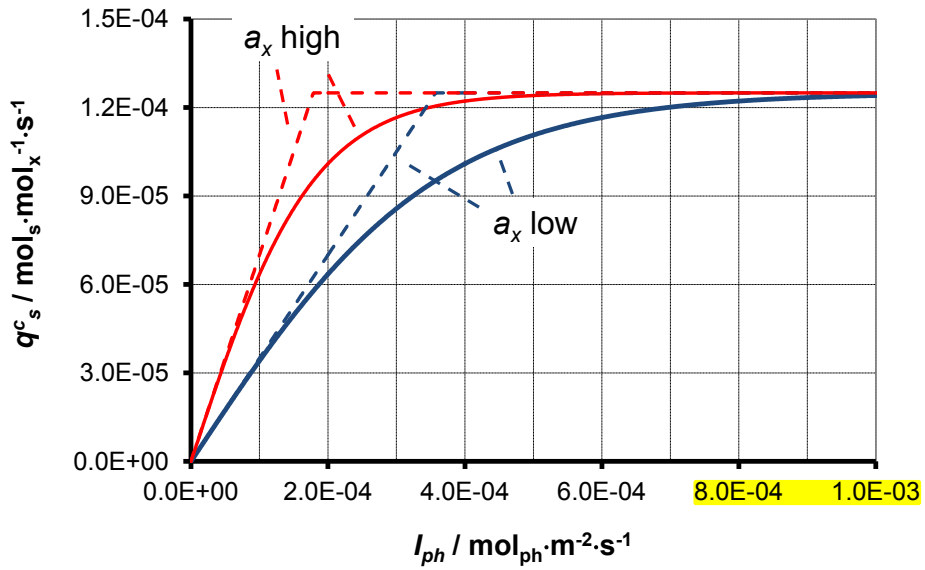

Figure 13: The specific rate of photosynthesis as a function of photon flux density I_{ph}. Photosynthesis is represented by the specific sugar production rate in the chloroplast q^c_s. Two models are shown: Jassby & Platt (solid lines) and Blackman (dashed lines). The curves in red reflect the behaviour of microalgal cells acclimated to low photon flux density having high pigment content, and thus high a_x. The curves in blue reflect the behaviour of microalgal cells acclimated to high photon flux density having low pigment content, and thus low a_x. Parameter values based on *Chlorella sorokiniana*: a_x = 3.5 m^2·mol$_x^{-1}$ (high light); a_x = 7.0 m^2·mol$_x^{-1}$ (low light); $Y^c_{s/ph,m}$ = 0.10 mol$_s$·mol$_{ph}^{-1}$; $q^c_{s,m}$ = 1.25·10^{-4} mol$_s$·mol$_x^{-1}$·s^{-1}; M_x = 24 g·mol$_x^{-1}$.

In Figure 13 the photosynthesis response according to both models (Blackman and Jassby & Platt) are shown. As discussed before microalgae will acclimate to the light conditions experienced. In case the algae are light limited they will respond by increasing their pigmentation and, as such, their specific light absorption coefficient a_x. This process is called photoacclimation. It has implications for the photosynthetic rates at low photon flux density. Cells with a large a_x will absorb more light and will thus express a higher photosynthetic rate under light limited conditions[1].

The photosynthetic response shown in Figure 12 and Figure 13 represent instantaneous rates of microalgae acclimated to a certain photon flux density and it is thus assumed that a_x is constant. In the situation microalgal cells acclimated to light-limited (low light) conditions would be transferred to a high photon flux density they would slowly decrease their pigment content and thus a_x. This acclimation process takes many hours.

Comparison photosynthesis models

The model of Jassby & Platt is reported to best describe of the photosynthetic response to light (Jassby & Platt 1976; Chalker 1980). In this chapter the model of Jassby & Platt will be used to evaluate microalgal growth in photobioreactors, but also the simpler Blackman model. The Blackman model can be easily solved analytically and is well suited to highlight and discuss the specific aspects of phototrophic production processes. Besides these two models there are alternative models. Two models which are frequently used are the model of Webb and a Monod model:

The model of Webb:

$$q_s^c = q_{s,m}^c \cdot \left(1 - e^{\left(\frac{-\alpha \cdot I_{ph}}{q_{s,m}^c}\right)}\right)$$

A Monod model:

$$q_s^c = q_{s,m}^c \cdot \frac{I_{ph}}{K_s + I_{ph}} \qquad K_s = \frac{q_{s,m}^c}{\alpha}$$

And thus:

$$q_s^c = q_{s,m}^c \cdot \frac{I_{ph}}{\frac{q_{s,m}^c}{\alpha} + I_{ph}}$$

Also in these models:

$$\alpha = a_x \cdot Y_{s/ph,m}^c$$

[1] Light limitation is defined as a photon flux density under which the maximal rate of photosynthesis is not reached yet, and no other nutrients are limiting growth.

In Figure 14 all 4 models introduced are compared. The parameters α and $q^c_{s,m}$ are chosen equal for all 4 models because these represent inherent biological characteristics. Only the model of Jassby & Plat is able to accurately describe the real (measured) photosynthesis response on light (as demonstrated in Figure 15). The model of Webb is 2nd best and is used frequently in microalgal research. When comparing the model of Webb with the model of Jassby & Platt it can be seen that the rate of photosynthesis levels of too rapidly when increasing photon flux density. The Monod model is used in modelling of other bioprocesses but it levels of even more rapidly.

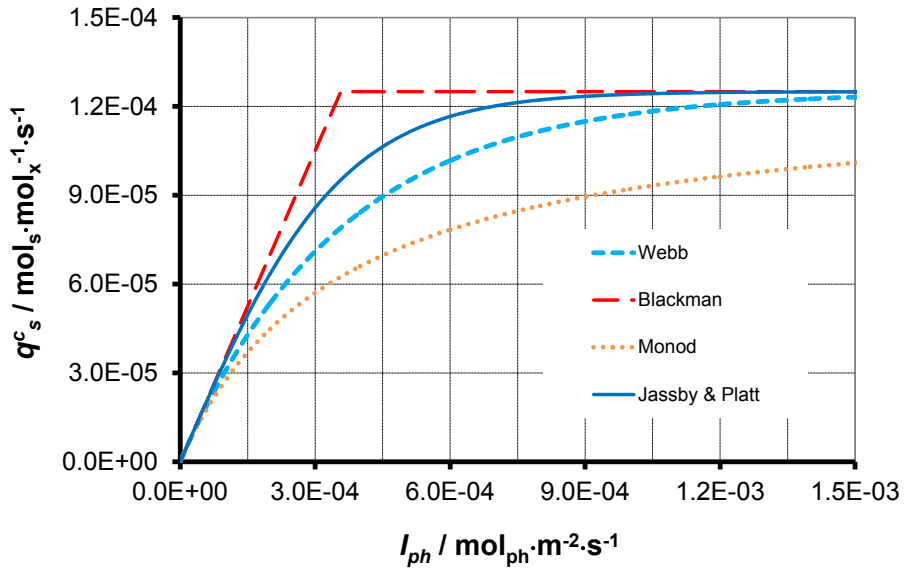

Figure 14: Comparison photosynthesis models. Parameter values based on high-light acclimated *Chlorella sorokiniana*: a_x = 3.5 m^2·mol$_x^{-1}$; $Y^c_{s/ph,m}$ = 0.10 mol$_s$·mol$_{ph}^{-1}$; $q^c_{s,m}$ = 1.25·10^{-4} mol$_s$·mol$_x^{-1}$·s^{-1}; M_x = 24g·mol$_x^{-1}$.

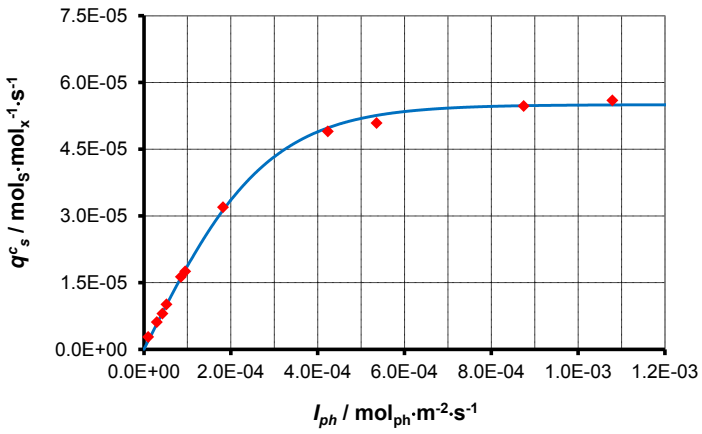

Figure 15: Curve-fit of the model of Jassby & Platt to the photosynthesis response on increasing photon flux density as measured for the green microalga *Chlamydomonas reindhardtii*. Data derived from measurements by Vejrazka et al (Vejrazka et al. 2013).

mS = specific sugar consumption rate for maintenance [molS·molx-1·s-1]
Yx/s = yield of biomass on sugar (CH2O)
μ = specific growth rate
qs = specific sugar (CH2O) consumption rate in microalgal cell

2.3 Microalgal growth

Microalgal growth can be coupled to photosynthetic sugar production employing a simple substrate balance according to Pirt (Pirt 1965). The specific consumption rate of sugar outside of the chloroplast q_s (unit $mol_S \cdot mol_x^{-1} \cdot s^{-1}$) then can be coupled to the specific growth rate μ (unit s^{-1}) of the microalgae.

$$q_s = -\frac{\mu}{Y_{x/s}} - m_s \qquad [mol_s \cdot mol_x^{-1} \cdot s^{-1}]$$

This relation can be rewritten to obtain a function to calculate the specific growth rate.

$$\mu = \left(-q_s - m_s\right) \cdot Y_{x/s} \qquad [s^{-1}]$$

Moreover, it was already discussed that the specific consumption rate of sugar (CH_2O) is directly to its production in the chloroplast q^c_s.

$$-q_s = q_s^c \qquad [mol_s \cdot mol_x^{-1} \cdot s^{-1}]$$

This results in a final expression for teh specific growth rate.

$$\mu = \left(q_s^c - m_s\right) \cdot Y_{x/s} \qquad [s^{-1}]$$

Please note that the maximal specific growth rate μ_m of a microalgal species can be described as a function of the maximal rate of photosynthesis $q^c_{s,m}$:

$$\mu_m = \left(q_{s,m}^c - m_s\right) \cdot Y_{x/s}$$

The variable q^c_s depends on the photon flux density I_{ph} as discussed in the previous section where the photosynthesis models of Jassby & Platt and Blackman were introduced. Consequently, the specific growth rate μ can be written as a function of the photon flux density as illustrated in Figure 16.

$$\mu = f(I_{ph}) = \left(q_s^c(I_{ph}) - m_s\right) \cdot Y_{x/s}$$

Not surprisingly, the relation between specific growth rate and photon flux density has an almost identical shape as the relation between the specific rate of photosynthesis and photon flux density. But, because of the maintenance requirement for sugar m_s there will be 'negative growth' in darkness meaning that sugar reserves are slowly depleted. In order to achieve positive growth the photon flux density I_{ph} needs to be higher than the so-called compensation point of photoautotrophic growth $I_{ph,c}$. At this photon flux density $I_{ph,c}$ just enough sugar is produced in the chloroplast to compensate for the amount lost due to cellular maintenance. The existence of the compensation point is illustrated in the insert of Figure 16.

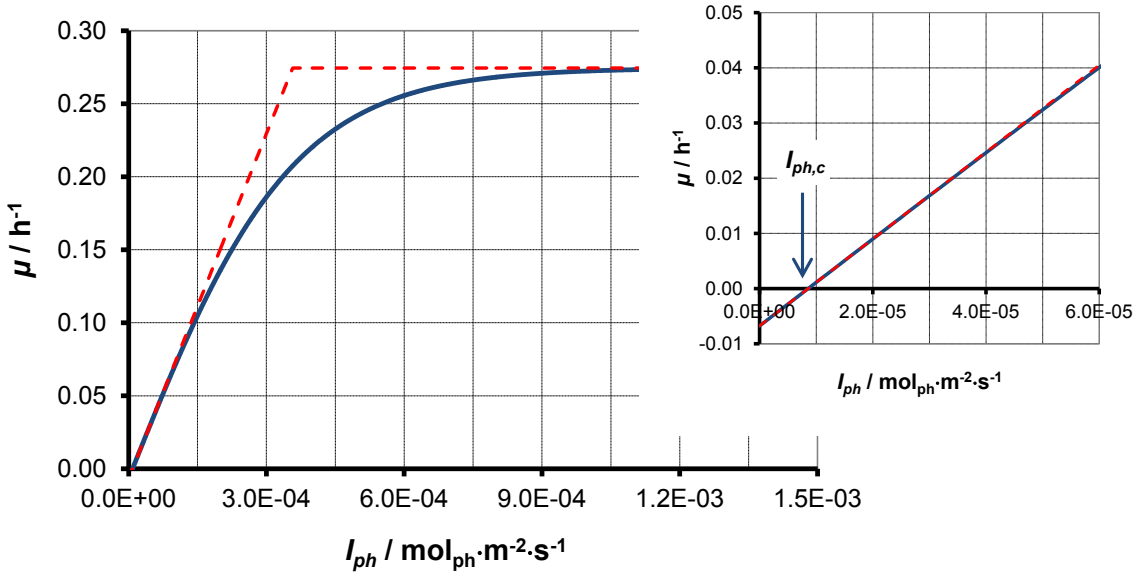

Figure 16: Specific growth rate μ of a microalga as a function of photon flux density I_{ph}. The specific growth rate is derived from Pirt's law in combination with the photosynthesis models of Jassby & Platt (solid line) or Blackman (dashed line). The insert illustrates the compensation point $I_{ph,c}$ where photosynthesis q^c_s is compensated by maintenance associated respiration m_s. Parameter values based on high-light acclimated *Chlorella sorokiniana*: a_x = 3.5 $m^2 \cdot mol_x^{-1}$; $Y^c_{s/ph,m}$ = 0.10 $mol_s \cdot mol_{ph}^{-1}$; $q^c_{s,m}$ = 1.25·10^{-4} $mol_s \cdot mol_x^{-1} \cdot s^{-1}$; $Y_{x/s}$ = 0.625 $mol_x \cdot mol_s^{-1}$; m_s = 3.0·10^{-6} $mol_s \cdot mol_x^{-1} \cdot s^{-1}$; M_x = 24 $g \cdot mol_x^{-1}$.

Based on the Blackman model the compensation point $I_{ph,c}$ can be calculated.

When $I_{ph} = I_{ph,c}$, then $\mu = 0$, and thus:

$$0 = \left(q_s^c(I_{ph,c}) - m_s\right) \cdot Y_{x/s} \Leftrightarrow q_s^c(I_{ph,c}) = m_s \qquad [mol_s \cdot mol_x^{-1} \cdot s^{-1}]$$

Please note that $I_{ph,c} < I_{ph,s}$ and according to the Blackman model:

$$q_s^c(I_{ph,c}) = \alpha \cdot I_{ph,c} = Y^c_{s/ph,m} \cdot a_x \cdot I_{ph,c} \qquad [mol_s \cdot mol_x^{-1} \cdot s^{-1}]$$

Combining both relations for $q_s^c(I_{ph,c})$ gives:

$$m_s = Y^c_{s/ph,m} \cdot a_x \cdot I_{ph,c} \qquad [mol_s \cdot mol_x^{-1} \cdot s^{-1}]$$

Further re-writing gives the final expression for $I_{ph,c}$:

$$I_{ph,c} = \frac{m_s}{Y^c_{s/ph,m} \cdot a_x} \qquad [mol_{ph} \cdot m^{-2} \cdot s^{-1}]$$

Iph,c = compensation photon flux density for photoautotrophic growth

Iph = PAR photon flux density

qcs = specific sugar (CH2O) production rate in chloroplast

Iph,s = saturation photon flux density for photosynthesis

Yc s/ph,m = maximal yield of sugar (CH2O) produced on photons

Definition of *instantaneous* specific growth rate μ_{PI}

On a time scale of several hours microalgae will acclimate to prevailing light conditions by modifying their pigment content and their specific light absorption coefficient (i.e. optical cross section). This process is called photoacclimation. Light limited microalgae will respond by increasing their pigmentation and, as such, their specific absorption coefficient a_x. Cells with a large a_x will absorb more light and will thus express a higher photosynthetic rate q^c_s under light limited conditions. High-light acclimated cells will give the opposite response.

Because the specific growth rate μ of microalgae is directly related to the rate of photosynthesis q^c_s, also the specific growth rate is affected by the acclimation-state of the microalgae. It might seem very strange that there are multiple relations between specific growth rate and photon flux density: a different one for every possible value of the specific absorption coefficient a_x (see Figure 17). But, this is the situation which needs to be considered.

ax = spectrally-averaged specific light absorption coefficien

photosynthetic rate = qc s = specific sugar (CH2O) production rate in chloroplast

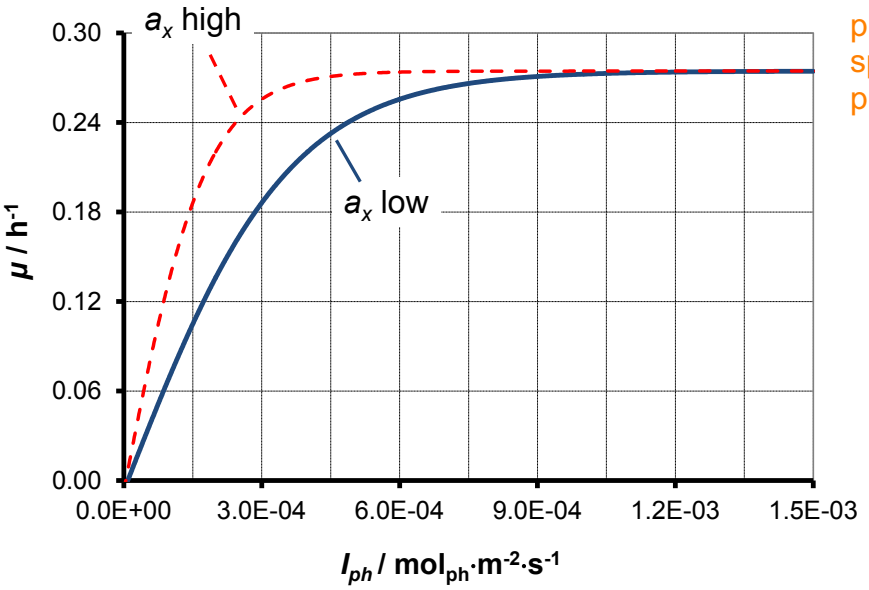

Figure 17: Instantaneous specific growth rate μ_{PI} of a microalga as a function of photon flux density I_{ph} and the influence of photoacclimation. The specific growth rate is derived from Pirt's law in combination with the photosynthesis models of Jassby & Platt. Parameter values based on *Chlorella sorokiniana*: a_x = 3.5 m^2·mol$_x^{-1}$ (high light); a_x = 7.0 m^2·mol$_x^{-1}$ (low light); $Y^c_{s/ph,m}$ = 0.10 mol$_s$·mol$_{ph}^{-1}$; $q^c_{s,m}$ = 1.25·10^{-4} mol$_s$·mol$_x^{-1}$·s^{-1}; $Y_{x/s}$ = 0.625 mol$_x$·mol$_s^{-1}$; m_s = 3.0·10^{-6} mol$_s$·mol$_x^{-1}$·s^{-1}; M_x = 24 g·mol$_x^{-1}$.

As will be discussed elsewhere in this chapter microalgae are usually grown in dense cultures inside photobioreactors or raceway ponds. Consequently, microalgae will shade each other. Microalgae will

experience maximal light levels at the light exposed surface of the culture and they will experience low light levels, or even darkness, at the bottom. In other words, they will experience a different photon flux density depending on their position within the culture. Due to mixing of the culture microalgae will then be temporarily exposed to different light levels. Depending on the cultivation system mixing times over this light gradient may vary from a few seconds, to multiple seconds, to minutes. The relation between the specific rate of photosynthesis and photon flux density proposed is very well suited to describe this temporal response within a microalgal culture.

$$\mu = \left(q_s^c(I_{ph}) - m_s\right) \cdot Y_{x/s}$$

This relation thus gives the specific growth rate of microalgae when the cells are temporarily exposed to a certain photon flux density at a certain location within a microalgal culture. The microalgae are acclimated to the 'average' light regime in the culture. On the long term (hours to days) they could change their acclimation state if for example the biomass density changes, or if the photon flux density at the surface changes.

For all these reasons the specific growth rate calculated from the specific rate of photosynthesis q^c_s will be called the instantaneous specific growth rate. The symbol μ_{PI} will be adopted for it. The subscript 'PI' reflects the relation between photosynthesis and photon flux density (irradiance) derived for q^c_s.

2.4 Energetic analysis of microalgal photosynthesis and growth

In Figure 18 the specific sugar production rate in the chloroplast q^c_s is plotted against the photon flux density I_{ph} according to the model of Jassby & Platt (solid line) as well as the model of Blackman (dashed line). In the same figure also the specific photon absorption rate q_{ph} is plotted. Specific photon absorption increases linearly with the photon flux density the microalgae are exposed to according to the following relationship:

$$-q_{ph} = a_x \cdot I_{ph}$$

Please note that a minus sign is added to q_{ph} because actual absorption (consumption) has a negative value. In contrast to the linear increase of $-q_{ph}$, the rate of photosynthesis q^c_s levels off and reaches a maximal level $q^c_{s,m}$. It is evident from figure 24 that at increasing photon flux density a discrepancy develops between photosynthesis q^c_s and light absorption q_{ph}.

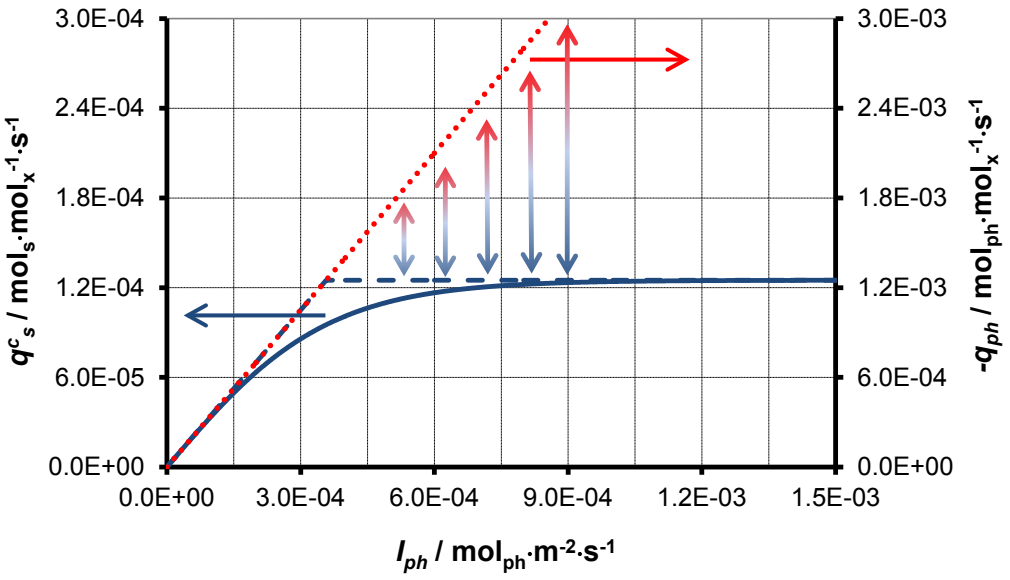

Figure 18: Specific rate of sugar production q^c_s (bleu lines) and light absorption $-q_{ph}$ (dotted red line) as a function of photon flux density I_{ph}. The solid blue line follows the model of Jassby & Platt, the dashed blue line follows the Blackman model. The double-sided arrows exemplify the mismatch between light use and light absorption at increasing photon flux density. Parameter values based on high-light acclimated *Chlorella sorokiniana*: a_x = 3.5 m^2·mol$_x^{-1}$; $Y^c_{s/ph,m}$ = 0.10 mol$_s$·mol$_{ph}^{-1}$; $q^c_{s,m}$ = 1.25·10^{-4} mol$_s$·mol$_x^{-1}$·s^{-1}; M_x = 24 g·mol$_x^{-1}$. Please note that the scale of the q_{ph}-axis is exactly 10 times higher and that the maximal yield of sugar on photons $Y^c_{s/ph,m}$ is 0.10 mol$_s$·mol$_{ph}^{-1}$. Both facts combined explain the fact that at low photon flux density both curves have the same slope.

Solely focusing on what is happening in photosynthesis in the chloroplast the observable yield of sugar on photons absorbed $Y^c_{s/ph}$ according to the following relation:

$$Y^c_{s/ph} = \frac{q^c_s}{-q_{ph}} \qquad [\text{mol}_s\cdot\text{mol}_{ph}^{-1}]$$

This observable yield is different from the maximal yield of sugar on photons $Y_{s/ph,m}$ which was defined earlier and which is one of the parameters in the photosynthesis models. This observable yield is a measure of the actual efficiency at which light energy is used in photosynthesis. In Figure 19 it can be seen that when the photon flux density I_{ph} approaches 0 mol$_{ph}$·m^{-2}·s^{-1} the maximal yield of 0.10 mol$_s$·mol$_{ph}^{-1}$ is reached.

On the contrary, at increasing photon flux density the yield drops and only part of the photons absorbed are really used in photosynthesis. The surplus of light absorbed by the pigments in the photosystems is dissipated as heat by the same photosystems. Dedicated biochemical and biophysical processes inside the photosystems and their pigments make this possible (Müller et al.

2001; Foyer et al. 2012). In this way the surplus of light can be safely disposed of. This decrease in the efficiency of photosynthesis at increasing photon flux density is called photosaturation, or light saturation.

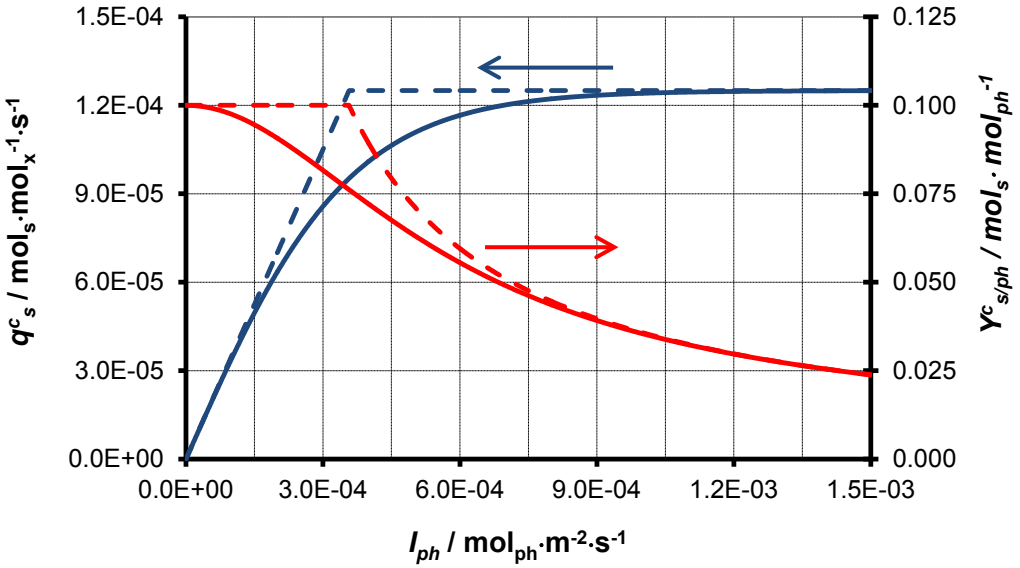

Figure 19: Specific rate of sugar production q^c_s (bleu lines) and the observable yield of sugar on photons absorbed $Y^c_{s/ph}$ (red lines) as a function of photon flux density I_{ph}. The solid lines follow the model of Jassby & Platt, the dashed lines follow the Blackman model. Parameter values based on high-light acclimated *Chlorella sorokiniana*: a_x = 3.5 m^2·mol$_x^{-1}$; $Y^c_{s/ph,m}$ = 0.10 mol$_s$·mol$_{ph}^{-1}$; $q^c_{s,m}$ = 1.25·10^{-4} mol$_s$·mol$_x^{-1}$·s^{-1}; M_x = 24 g·mol$_x^{-1}$.

Similarly, also the observable yield of biomass on photons absorbed can be calculated:

$$Y_{x/ph} = \frac{\mu_{Pl}}{-q_{ph}} \qquad [\text{mol}_x \cdot \text{mol}_{ph}^{-1}]$$

$$\Leftrightarrow Y_{x/ph} = \frac{\left(q_s^c - m_s\right) \cdot Y_{x/s}}{-q_{ph}} \qquad [\text{mol}_x \cdot \text{mol}_{ph}^{-1}]$$

The symbol μ_{Pl} thus reflects the instantaneous specific growth rate as calculated from the specific rate of photosynthesis q^c_s.

The relation between observable biomass yield on photons and photon flux density is shown in Figure 20. Similar to the sugar yield also the biomass yield on photons absorbed $Y_{x/ph}$ decreases at increasing photon flux density because of the photosaturation effect. At low photon flux density a different trend is observed. The biomass yield does not increase to a maximal value when I_{ph} approaches 0 mol$_{ph}$·m^{-2}·s^{-1}. On the contrary, $Y_{x/ph}$ drops dramatically at very low light levels. This is

related to the fact that the larger part of the little light absorbed must be used for cellular maintenance. Sugars are still produced at high efficiency by photosynthesis in the chloroplast, but almost all sugar is broken down again to provide energy for maintenance. Consequently, little or no energy is left for biomass growth.

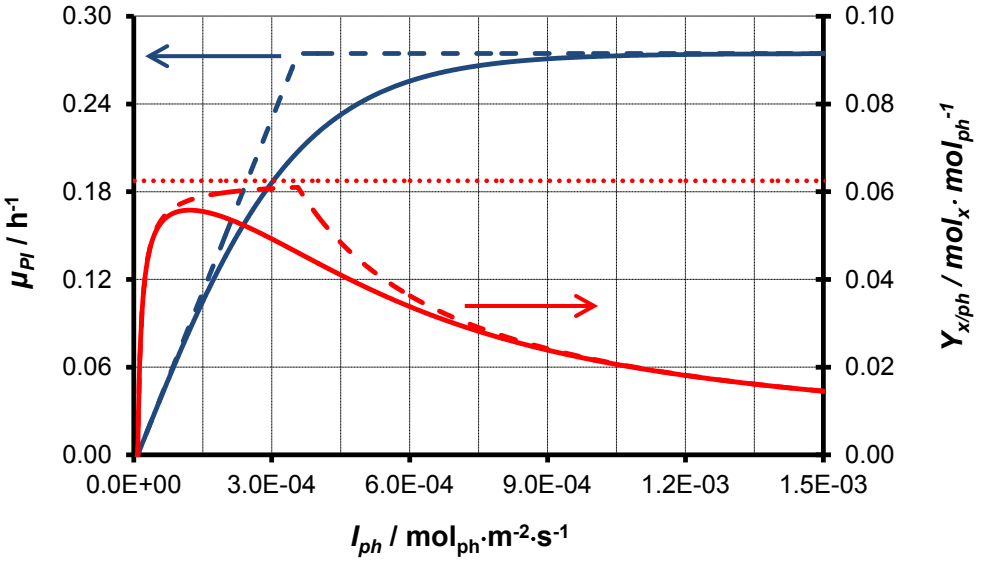

Figure 20: Instantaneous specific growth rate μ_{PI} (bleu lines) and the observable yield of biomass on photons $Y_{x/ph}$ (red lines) as a function of photon flux density I_{ph}. The solid lines follow the model of Jassby & Platt, the dashed lines follow Blackman. The dotted red line represents the hypothetical maximal biomass yield on photons $Y_{x/ph,m}$ when maintenance requirement is neglected (m_s = 0). Parameter values based on high-light acclimated *Chlorella sorokiniana*: a_x = 3.5 $m^2 \cdot mol_x^{-1}$; $Y^c_{s/ph,m}$ = 0.10 $mol_s \cdot mol_{ph}^{-1}$; $q^c_{s,m}$ = $1.25 \cdot 10^{-4}$ $mol_s \cdot mol_x^{-1} \cdot s^{-1}$; $Y_{x/s}$ = 0.625 $mol_x \cdot mol_s^{-1}$; m_s = $3.0 \cdot 10^{-6}$ $mol_s \cdot mol_x^{-1} \cdot s^{-1}$; M_x = 24 $g \cdot mol_x^{-1}$.

In a hypothetical situation where the cells have no maintenance requirements (m_s = 0) the maximal biomass yield can be calculated as follows:

$$Y_{x/ph,m} = Y^c_{a/ph,m} \cdot Y_{x/s}$$

The dotted horizontal line in Figure 20 represents this hypothetical maximum which cannot be reached in practice. In the example presented in Figure 20 it was assumed that the biomass yield on sugar was 0.625 $mol_x \cdot mol_s^{-1}$ and that the sugar yield on photons was 0.10 $mol_s \cdot mol_{ph}^{-1}$, and thus:

$$Y_{x/ph,m} = 0.10 \cdot 0.625 = 0.0625 \qquad [mol_x \cdot mol_{ph}^{-1}]$$

Knowing that the weight of 1 C-mol of biomass (i.e.1 mol_x) equals about 24 grams this means that 1 mol of PAR photons can be converted in 1.50 grams of biomass in the hypothetical situation

maintenance can be neglected. In practice maintenance will reduce the yield on photons as illustrated by the model description presented in Figure 20 where the maximal yield $Y_{x/ph,m}$ is not reached.

It must be noted that this value for $Y_{x/ph,m}$ is an estimate because the yield of biomass on sugar $Y_{x/s}$ is usually not well known and this was already discussed before. Also the value of the maximal yield of sugar on photons $Y_{s/ph,m}$ was discussed before and it was shown that its value is close to 0.10 mol $mol_s \cdot mol_{ph}^{-1}$. The spectral dependence of the yield of photosynthesis $Y^c_{s/ph,m}$ was not discussed yet. In the old work of Emerson and Lewis, and in the work of Tanada (Emerson & Lewis 1943; Tanada 1951) the spectral dependency of the yield of photosynthesis is described and some of their data are re-drawn and presented in Figure 21. Blue light (400-500 nm) appears to be used with a reduced efficiency. In the green part of the spectrum (500-600 nm) the efficiency increases up to a maximal level observed in the red region (600-700 nm). It is important to emphasize that the efficiency in the blue and green region still is still more than 70% of the level in the red region. Within the framework of a simple model description for engineering purposes we propose we can assume a flat spectral response in the PAR range and thus assume a fixed sugar yield on photons irrespective of the wavelength.

The studies of Emerson and Lewis and Tanada already date from the middle of last century. Almost no attempts have been made to measure the spectral dependence of the efficiency of photosynthesis with latest technology, or with other microalgal species. Only recently a new approach was presented by Tamburic and co-workers (Tamburic et al. 2014) for the marine eustigmatophyte microalga *Nannochloropsis*. This study confirms that all wavelengths across the PAR spectrum can be utilized with similar efficiency to drive photosynthesis. Although Tamburic reported differences between certain wavelengths the lowest values measured were still 70% of the maximal values and no consistent differences between the blue, green, and red spectral regions were reported.

Within the research arena of the higher plants (crop plants) much more work has been done on resolving the spectral dependency of the efficiency of light use in photosynthesis (Evans 1987; McCree 1971). The most recent study is the one of Hogewoning and co-workers (Hogewoning et al. 2012) who measured the maximal yield of carbon dioxide (CO_2) fixation in cucumber leaves as a function of wavelength. CO_2 fixation in the chloroplasts is equivalent to sugar production. Hogewoning measured a yield of CO_2 fixation on photons between 0.06 and 0.09 $mol_{CO2} \cdot mol_{ph}^{-1}$. The lower value of

0.06 was measured in the bleu range (400-500 nm) and the higher value of 0.09 in the red range (600-700 nm). In the green part of the spectrum the yield increased from 0.06 $mol_{CO2} \cdot mol_{ph}^{-1}$ at 500 nm to 0.09 $mol_{CO2} \cdot mol_{ph}^{-1}$ at 600 nm. The lower yield in the blue range can be largely explained by the absorption of non-photosynthetic pigments which attributed to about 20% of the total light absorption between 400 and 500 nm. The work of Hogewoning thus confirms the old work Emerson and Lewis on *Chlorella* (Figure 21).

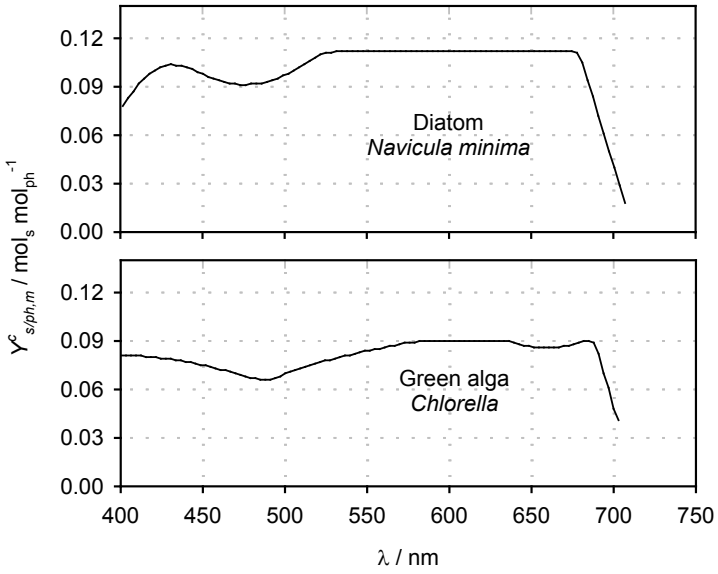

Figure 21: Maximum yield of sugar on photons in the chloroplast $Y^c_{s/ph,m}$ as a function of wavelength λ. $Y^c_{s/ph,m}$ is shown for a green alga, *Chlorella* (Emerson & Lewis 1943); and a diatom, *Navicula minima* (Tanada 1951).

From biomass yield on photons to *photosynthetic efficiency*

Commonly the potential of large-scale microalgae production is supported by referring to their high 'photosynthetic efficiency' (*PE*). This efficiency is based on the fraction of light energy (%) stored as the chemical energy within the biomass. The biomass yield on photons is expressed as a mole fraction ($mol_x \cdot mol_{ph}^{-1}$) but can be converted into energy units taking into account the energy content of the photons as well as the energy content of the biomass. The results of such recalculations are shown in Table 1 while assuming different values for the maximal sugar yield on photons $Y_{s/ph,m}$, and the biomass yield on sugar $Y_{x/s}$. The calculations are based on microalgae cultivated under nutrient-replete and thus light-limited conditions.

Based on the assumption that 10 photons are required for the production of 1-carbon equivalent of sugar ($Y_{s/ph,m}$ = 0.10 $mol_s \cdot mol_{ph}^{-1}$) the photosynthetic efficiency of microalgal growth ranges between 5.5 and 7.7% depending on the assumed biomass yield on sugar ($Y_{x/s}$). The higher value of 7.7% corresponds to a biomass yield on sugar of 0.7 $mol_x \cdot mol_s^{-1}$, which would be among the highest reported for aerobic chemoheterotrophic growth. When normalizing to the PAR range of 400 to 700 nm the photosynthetic efficiency ranges between 12.9 and 18.1% depending on $Y_{x/s}$. When narrowing down to the minimal band-gap required by photosystem II (i.e. 680 nm) the efficiency ranges between 15.9 and 22.2% depending on the value of $Y_{x/s}$.

Table 1: Maximal biomass yield on photons, and maximal photosynthetic efficiency (PE) of photoautotrophic microalgal growth under nutrient-replete conditions. Numbers used: PAR fraction sunlight: 42.3% (based on ASTM g173 spectrum); Energy content PAR photons sunlight: 216 $KJ \cdot mol_{ph}^{-1}$ (based on ASTM g173 spectrum); molar weight of biomass (1-carbon equivalent): M_x = 24 $g \cdot mol_x^{-1}$; Enthalpy of combustion biomass: $\Delta H_c^0(s)$ = 559 $KJ \cdot mol_x^{-1}$; degree of reduction biomass: γ = 4.86; molar weight of sugar (CH_2O): M_x = 30 $g \cdot mol_x^{-1}$; enthalpy of combustion sugar: $\Delta H_c^0(s)$ = 460 $KJ \cdot mol_x^{-1}$; degree of reduction sugar: γ = 4 References: (Cordier et al. 1987; Kliphuis et al. 2010; Kliphuis et al. 2012; Kliphuis, Martens, et al. 2011).

$Y_{s/ph,m}$	$Y_{x/s}$	$Y_{x/ph}$		*PE / %*		
$mol_s \cdot mol_{ph}^{-1}$	$mol_x \cdot mol_s^{-1}$	$mol_x \cdot mol_{ph}^{-1}$	$g \cdot mol_{ph}^{-1}$	*680 nm*	*sunlight PAR*	*sunlight complete*
0.100	0.5	0.050	1.20	15.9%	12.9%	5.5%
	0.6	0.060	1.44	19.1%	15.5%	6.6%
	0.7	0.070	1.68	22.2%	18.1%	7.7%
	sugar (CH_2O) only →		*3.00*	*26.2%*	*21.3%*	*9.0%*
0.125	0.5	0.0625	1.50	19.8%	16.2%	6.8%
	0.6	0.075	1.80	23.8%	19.4%	8.2%
	0.7	0.0875	2.10	27.8%	22.6%	9.6%
	sugar (CH_2O) only →		*3.75*	*32.7%*	*26.6%*	*11.3%*

The higher values of the biomass yield on sugar $Y_{x/s}$ probably can only be reached with ammonium or urea as a nitrogen source. In that situation the actual energy stored in the overall reaction representing microalgal growth is less than the enthalpy of combustion of biomass. This is related to the fact that the enthalpy of combustion of these reduced nitrogen compounds is considerable. Taking this into

account maximal PE will drop will drop from 7.7% to 7.1% (assuming $Y_{s/ph,m}$ = 0.1 $mol_s \cdot mol_{ph}^{-1}$ and $Y_{x/s}$ = 0.7 $mol_x \cdot mol_s^{-1}$). Moreover, in real microalgae production systems standing biomass will continuously consume photosynthetically derived sugar for maintenance purposes bringing down maximal PE further. This effect will be exemplified in the following section on photobioreactor productivity.

In the hypothetical situation that only 8 photons are required for the production of 1-carbon equivalent of sugar ($Y_{s/ph,m}$ = 0.125 $mol_s \cdot mol_{ph}^{-1}$) the photosynthetic efficiency of microalgal growth ranges between 6.8 and 9.6% depending on the assumed biomass yield on sugar ($Y_{x/s}$). Statements of *PE* for microalgae production beyond 9.6% should thus be treated with great caution as it is very unlikely that the $Y_{x/s}$ is higher than 0.7. Moreover, as discussed before, the yield of sugar on photons achieved under ideal conditions is closer to 0.10 than 0.125 $mol_s \cdot mol_{ph}^{-1}$. Possibly statements of PE of 10%, or more, could be based on the first steps of photosynthesis leading to the production of sugar. In an extra calculation included in Table 1 is referred to a hypothetical situation microalgal cells are only producing and accumulating sugar (CH_2O). In that case a maximal PE on sunlight of 11.3% can be reached.

3 Estimating photobioreactor productivity

There is a wide variety photobioreactors ranging from closed photobioreactors of variable designs to open microalgal raceway ponds. The productivity of such photobioreactors will be analyzed in a general way under the assumption that they are operated under light limited conditions. In other words it is assumed assume that all nutrients, including carbon dioxide, are available in excess. In addition, it is assumed that all culture parameters are maintained at their optimal range, e.g. pH, temperature, salinity, dissolved oxygen concentration.

3.1 Light penetration in microalgal cultures

Microalgae absorb light and, consequently, the photon flux density will decrease along the path light takes through a microalgal culture. In order to quantify microalgal growth in photobioreactors the local photon flux density within the microalgal culture must be known. The specific light absorption coefficient $a_{x,\lambda}$ of the microalgae can be used to calculate light penetration. Its value is wavelength-dependent meaning that light of certain wavelengths are absorbed more strongly than others.

For simplicity it is assumed that the effect of light scattering can be neglected. Later this simplification will be re-visited and the effect of light scattering will be discussed in general terms. In the analysis to follow a uni-directional light field is assumed which is perpendicular to a flat light-exposed surface, e.g. raceway ponds or panel-type photobioreactors. In that case the Law of Lambert-Beer can be used to calculate the photon flux density $I_{ph,\lambda}(z)$ at each location z within the microalgal culture. Lambert-Beer states that the attenuation of light over an infinitesimal small distance is proportional to the photon flux density itself.

$$\frac{dI_{ph,\lambda}}{dz} = -a_{x,\lambda} \cdot C_x \cdot I_{ph,\lambda}$$

The proportionality constant is the product of the biomass concentration C_x and the specific light absorption coefficient $a_{x,\lambda}$ (i.e. the optical cross section). Integrating from the light exposed surface (z = 0) to any location z then delivers an exponential decrease of the photon flux density over z.:

$$I_{ph,\lambda}(z) = I_{ph,\lambda}(0) \cdot e^{-a_{x,\lambda} \cdot C_x \cdot z} \qquad [\mathrm{mol_{ph} \cdot m^{-2} \cdot s^{-1} \cdot nm^{-1}}]$$

The photon flux density $I_{ph,\lambda}$ was introduced before and it represents the wavelength-dependent photon flux density with units $mol_{ph} \cdot m^{-2} \cdot s^{-1} \cdot nm^{-1}$. Its value at the light-exposed surface can be calculated as follows;

$$I_{ph,\lambda}(0) = I_{ph}(0) \cdot E_{n,\lambda} \qquad [mol_{ph} \cdot m^{-2} \cdot s^{-1} \cdot nm^{-1}]$$

The parameter $I_{ph}(0)$ represents the integrated photon flux density over the complete PAR range at the light-exposed surface of the photobioreactor. This parameter must be measured in order to estimate productivity of microalgal cultivation systems. It should be remembered that $E_{n,\lambda}$ (unit nm^{-1}) is the PAR-normalized spectrum of the light source used. More specifically, at each wavelength it gives the fraction of the total amount of PAR photons in a 1 nm interval explaining the unit nm^{-1}.

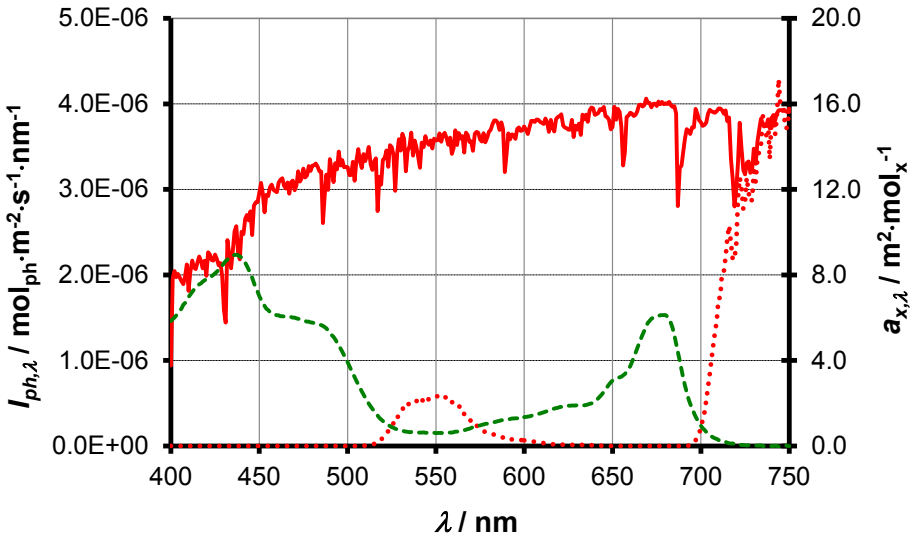

Figure 22: Light penetration in a microalgal culture according to Lambert-Beer as a function of the wavelength λ. The dashed green line is the specific light absorption coefficient $a_{x,\lambda}$. The solid red line represents the intensity of sunlight $I_{ph,\lambda}(0)$ at the light-exposed surface. The dotted red line represents the photon flux density $I_{ph,\lambda}$ in the microalgal culture at 0.03 m distance from the light-exposed surface. Parameter values based on high-light acclimated *Chlorella sorokiniana*: C_x = 100 $mol_x \cdot m^{-3}$; $I_{ph}(0)$ = $1 \cdot 10^{-3}$ $mol_{ph} \cdot m^{-2} \cdot s^{-1}$; a_x = 3.33 $m^2 \cdot mol_x^{-1}$; $E_{n,\lambda}$ for sunlight.

In the example shown in Figure 22 only a small part of green light is able to penetrate to the 'bottom' of the culture which is at 3 cm distance from the light exposed surface. Of course this depends on the actual biomass concentration C_x, which is 100 $mol_x \cdot m^{-3}$ in this example, and this is equivalent to 2.4 $kg \cdot m^{-3}$ (Mx ≈ 24 $g \cdot mol_x^{-1}$). It is apparent from the results presented in Figure 22 that also green light (500-600 nm) is largely absorbed in the culture and thus it is far from useless. In fact when referring to

Figure 21 and the concomitant discussion on the spectral dependence of the maximal yield of sugar on photons $Y^{c}_{s/ph,m}$ it is evident that green light is still used efficiently microalga; photosynthesis after it has been absorbed.

In order to calculate the integrated photon flux density over the complete PAR range at a depth *z* the contribution of all individual wavelengths from 400 to 700 nm have to be summed.

$$I_{ph}(z) = \sum_{400nm}^{700nm} I_{ph,\lambda}(0) \cdot e^{-a_{x,\lambda} \cdot C_x \cdot z} \cdot \Delta\lambda \qquad [mol_{ph} \cdot m^{-2} \cdot s^{-1}]$$

This approach can be simplified by adopting the spectrally-averaged specific absorption coefficient a_x.

$$I_{ph}(z) = I_{ph}(0) \cdot e^{-a_x \cdot C_x \cdot z} \qquad [mol_{ph} \cdot m^{-2} \cdot s^{-1}]$$

With:

$$a_x = \sum_{\lambda=400}^{\lambda=700} a_{x,\lambda} \cdot E_{n,\lambda} \cdot \Delta\lambda \qquad [m^2 \cdot mol_x^{-1}]$$

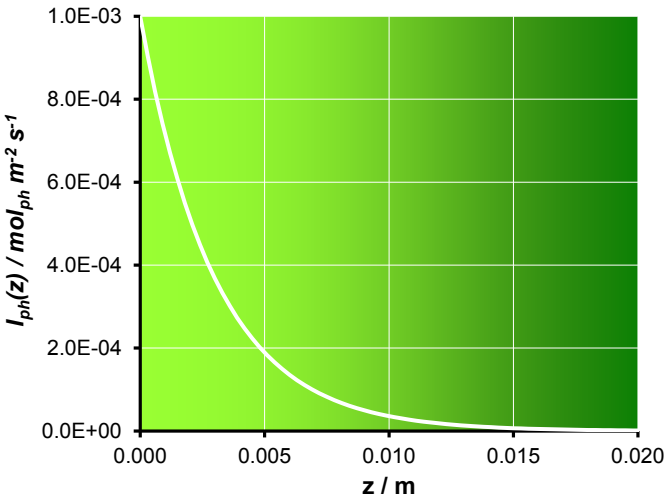

Figure 23: Light penetration in a microalgal culture neglecting wavelength dependency of light absorption, and thus assuming a constant a_x: I_{ph} as a function of depth *z*. The calculation of I_{ph} is based on Lambert-Beer with a constant specific light absorption coefficient a_x. Parameter values based on high-light acclimated *Chlorella sorokiniana*: a_x = 3.33 $m^2 \cdot mol_x^{-1}$; C_x = 100 $mol_x \cdot m^{-3}$; $I_{ph}(0)$ = $1 \cdot 10^{-3}$ $mol_{ph} \cdot m^{-2} \cdot s^{-1}$.

In theory an error is introduced when assuming a constant specific absorption coefficient a_x. This is related to the fact that the spectral distribution of light $E_{n,\lambda}$ changes when moving deeper inside a microalgal culture. This is also exemplified in Figure 22 where the spectrum changes from white (sunlight) at the reactor surface to green at the bottom. But, only by adopting this simplification later Lambert-Beer can be used in combination with the Blackman model to set up a complete model

description for photobioreactor productivity which can be readily solved. The result of this simplification is an exponential decrease of $I_{ph}(z)$ as a function of depth z as illustrated in Figure 23.

3.2 Microalgae cultivation in photobioreactors: calculating productivity

Photobioreactors usually are operated according to a chemostat mode (constant dilution) or turbidostat mode (constant turbidity) of operation. Details will be explained later in this chapter but below the biomass balance over a microalgal cultivation system is already presented:

$$V_r \cdot \frac{dC_x}{dt} = F_{in} \cdot C_{x,in} - F_{out} \cdot C_{x,out} + r_x \cdot V_r$$

With:

V_r	Liquid volume in photobioreactor	[m^3]
F_{in}/F_{out}	Liquid flow rate in and out of photobioreactor	[$m^3 \cdot s^{-1}$]
C_x	Biomass concentration in photobioreactor	[$mol_x \cdot m^{-3}$]
$C_{x,in}/C_{x,out}$	Biomass concentration in inflow or outflow	[$mol_x \cdot m^{-3}$]
r_x	Volumetric biomass production rate	[$mol_x \cdot m^{-3} \cdot s^{-1}$]

With respect to the design and operation of photobioreactors the production term r_x is of major importance. Parameter r_x represents the volumetric biomass production rate of a cultivation system and it is the product of the biomass concentration in the system and the average specific growth rate of the microalgae:

$$r_x = \bar{\mu} \cdot C_x \qquad [mol_x \cdot m^{-3} \cdot s^{-1}]$$

In order to assess the volumetric productivity of the system the microalgal biomass concentration and average specific growth rate need to be known. For the moment it will be assumed that the biomass concentration can be set at any desired level by means of a turbidostat mode of operation. Consequently, only the average specific growth rate of the microalgae in the photobioreactor needs to be calculated.

All theory necessary for this calculation is already introduced and is summarized in Figure 24. The photon flux density at any location z in the microalgal culture can be described with Lambert-Beer. Based on this local photon flux density the local specific rate of sugar production in the chloroplast (photosynthesis) can be calculated using photosynthesis models such as those of Jassby & Platt or Blackman. The local specific sugar production rates then can be integrated over culture depth to

obtain the average photosynthetic rate of the microalgal culture. Finally, based on the substrate balance for sugar (according to Pirt), the average specific growth rate of the microalgal culture can be calculated:

$$\overline{\mu} = \left(\overline{q_a^c} - m_a\right) \cdot Y_{x/a}$$

Below the calculation routines to calculate the average specific rate of sugar production in the chloroplast (photosynthesis) will be explained in more detail for the Blackman and Jassby & Platt models. In order to perform such calculations all necessary biological parameters must be known for the microalgal species to be cultivated: a_x; $Y^c_{s/ph,m}$; $q^c_{s,m}$; $Y_{x/s}$; m_s.

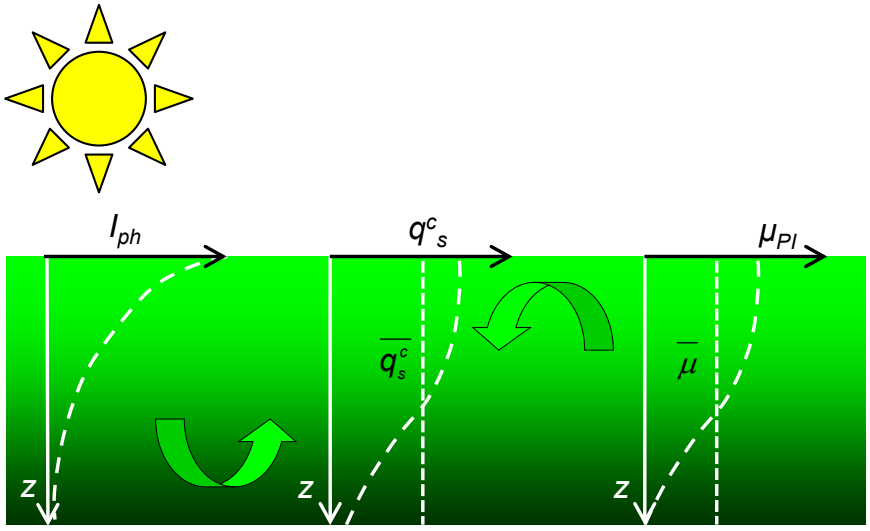

Figure 24: schematic drawing of the light gradient inside microalgal cultures and consequent gradients in specific rates. In the drawing three different graphs are included describing the dependency of the following parameters on the location z within the microalgal culture: (left) photon flux density I_{ph}; (middle) specific rate of photosynthesis q^c_s; (right) instantaneous specific growth rate μ_{Pl}.

Integrating photosynthesis along optical path according to Blackman

When adopting the Blackman model a simple but useful expression for the volumetric productivity of photobioreactors can be derived. In the Blackman model a constant specific light absorption coefficient is used. In other words, the change of light spectrum by preferential absorption within a microalgal culture is not included.

As discussed above the average specific sugar production rate of the microalgal culture must be calculated in order to asses photobioreactor volumetric productivity. The following integral therefore must be calculated:

$$\overline{q_s^c} = \frac{\int_o^d q_s^c(z) \cdot dz}{d}$$

$I_{ph}(z) \leq I_{ph,s}$: $\quad q_s^c = a_x \cdot Y_{s/ph,m} \cdot I_{ph}(z)$

$I_{ph}(z) \geq I_{ph,s}$: $\quad q_s^c = q_{s,m}^c$

The saturating photon flux density $I_{ph,s}$ can be calculated as follows:

$$I_{ph,s} = \frac{q_{CH2O,m}^c}{a_x \cdot Y_{CH2O/ph,m}^c}$$

Based on the biomass concentration C_x and the value $I_{ph,s}$ Lambert-Beer can be used to calculate the depth z inside the photobioreactor where the local photon flux density $I_{ph}(z)$ is equal to $I_{ph,s}$. This depth will be called the saturation depth z_s.

$I_{ph}(z_s) = I_{ph,s}$ and $I_{ph}(z_s) = I_{ph}(0) \cdot e^{-a_X \cdot C_X \cdot z_s}$

Combining these relations gives:

$$z_s = \frac{Ln\left(\frac{I_{ph}(0)}{I_{ph,s}}\right)}{a_x \cdot C_x}$$

Consequently, we can split up the photobioreactor in two zones (Figure 25):

1. $z = 0 \rightarrow z = z_s$ where $I_{ph}(z) \geq I_{ph,s}$, thus: $q_s^c = q_{s,m}^c$
2. $z = z_s \rightarrow z = d$ where $I_{ph}(z) \leq I_{ph,s}$, thus: $q_s^c = a_x \cdot Y_{s/ph,m} \cdot I_{ph}(z)$

Consequently the average specific sugar production rate of the microalgae can be described with the following integral:

$$\overline{q_s^c} = \frac{1}{d} \cdot \int_o^{z_s} q_{s,m}^c \cdot dz + \frac{1}{d} \cdot \int_{z_s}^d a_x \cdot Y_{s/ph,m}^c \cdot I_{ph}(z) \cdot dz$$

With: $I_{ph}(z) = I_{ph}(0) \cdot e^{-a_X \cdot C_X \cdot z}$

The analytical solution of this integral is:

$$\overline{q_s^c} = \frac{z_s}{d} \cdot q_{s,m}^c + \frac{Y_{s/ph,m}^c \cdot I_{ph}(0)}{d \cdot C_x}\left(e^{-a_X \cdot C_X \cdot z_s} - e^{-a_X \cdot C_X \cdot d}\right)$$

With: $z_s = \frac{Ln\left(\frac{I_{ph}(0)}{I_{ph,s}}\right)}{a_x \cdot C_x}$ and $I_{ph,s} = \frac{q_{s,m}^c}{a_x \cdot Y_{s/ph,m}^c}$

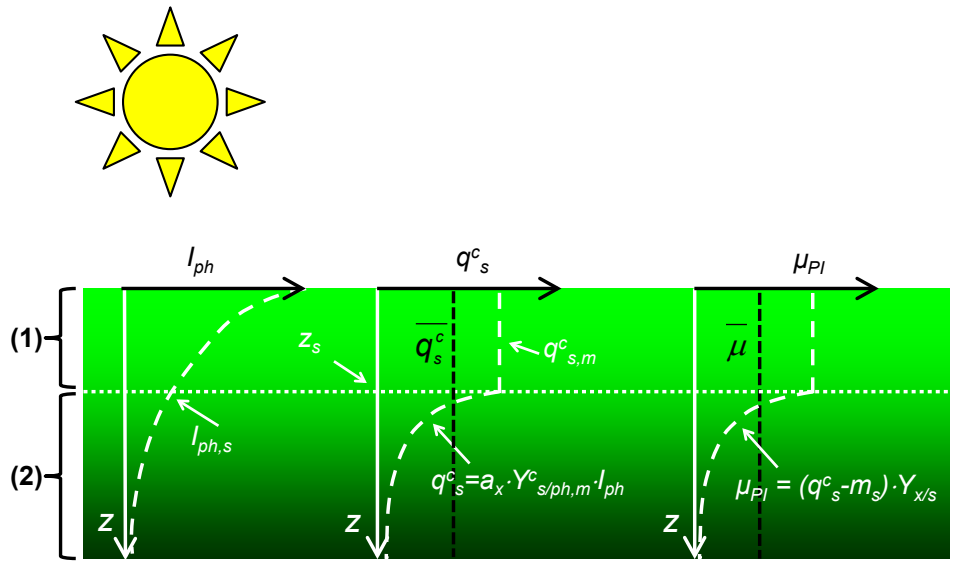

Figure 25: Schematic drawing of the light gradient inside microalgal cultures and the application of the Blackman model to calculate the average specific growth rate. The microalgal culture is subdivided in two zones: (1) $I_{ph}(z) \geq I_{ph,s}$; (2) $I_{ph}(z) \leq I_{ph,s}$. See Figure 24 for more details.

The following two special situations can occur:

$z_s \geq d$, and thus $I_{ph}(z) \geq I_{ph,s}$: $\overline{q^c_s} = q^c_{s,m}$

$I_{ph}(0) \leq I_{ph,s}$, and thus $z_s = 0$: $\overline{q^c_s} = \frac{Y^c_{s/ph,m} \cdot I_{ph}(0)}{d \cdot C_x}\left(1 - e^{-a_x \cdot C_x \cdot d}\right)$

Ultimately a single expression for the volumetric productivity of a microalgal culture in a photobioreactors can be derived:

$$r_x = \frac{Y_{x/s}}{d} \cdot \left\{ \frac{q^c_{s,m}}{a_x} \cdot \left(1 + Ln\left(\frac{I_{ph}(0) \cdot a_x \cdot Y^c_{s/ph,m}}{q^c_{s,m}} \right) \right) - Y^c_{s/ph,m} \cdot I_{ph}(0) \cdot e^{-a_x \cdot C_x \cdot d} \right\} - Y_{x/s} \cdot m_s \cdot C_x$$

This relation can be used for example to calculate volumetric productivity of a photbioreactor at different biomass concentrations C_x when assuming a constant incident photon flux density $I_{ph}(0)$. In Figure 26 results are shown for a photobioreactor with an optical depth of 3 cm. The shape of this relation will be discussed later after having introduced a similar approach based on the model of Jassby & Platt.

Integrating photosynthesis along optical path according to Jassby & Platt

The model of Jassby & Platt results in a more accurate description of the relation between the specific rate of photosynthesis (sugar production) and photon flux density. Again the average specific sugar production rate of the microalgal culture must be calculated in order to assess the volumetric productivity of a photobioreactor. The following integral therefore must be calculated:

$$\overline{q_s^c} = \frac{\int_o^d q_s^c(z) \cdot dz}{d}$$

$$q_s^c(z) = q_{s,m}^c \cdot \tanh\left(\frac{Y_{s/ph,m}^c \cdot a_x \cdot I_{ph}(z)}{q_{s,m}^c}\right)$$

The integral in this calculation routine cannot be easily solved, especially in the situation when also spectral dependence of light absorption must be taken into account. In that case we also have to include the relation below:

$$I_{ph}(z) = \sum_{400\,nm}^{700\,nm} I_{ph,\lambda}(0) \cdot e^{-a_{x,\lambda} \cdot C_X \cdot z} \cdot \Delta\lambda$$

For this reason, such problems nowadays are solved numerically using computational power. Already in simple spreadsheet programs such problems can be accurately solved by subdividing the photobioreactor in a large but finite number of layers and following below routine:

1. $I_{ph,\lambda}(0) = I_{ph}(0) \cdot E_{n,\lambda}$

2. $I_{ph}(z) = \sum_{400\,nm}^{700\,nm} I_{ph,\lambda}(0) \cdot e^{-a_{x,\lambda} \cdot C_X \cdot z} \cdot \Delta\lambda$

3. $q_{ph}(z) = \frac{I_{ph}(z + \frac{1}{2}\Delta z) - I_{ph}(z - \frac{1}{2}\Delta z)}{C_x \cdot \Delta z}$

4. $q_s^c(z) = q_{s,m}^c \cdot \tanh\left(\frac{Y_{s/ph,m}^c \cdot -q_{ph}(z)}{q_{s,m}^c}\right)$

5. $\overline{q_{Cs}^c} = \frac{\sum_{n=1}^{n=N} q_s^c(z) \cdot \Delta z}{d}$

In this approach it is assumed that q_{ph}, and q^c_s, are constant over the finite layer Δz. This assumption is only valid when the number of layers N is sufficiently large and Δz sufficiently small. In practice 100

layers within the photic zone[2] proves to be accurate. In this approach it is practical to express the specific rate of photosynthesis q^c_s based on the local specific photon consumption rate q_{ph}, and not based on the local photon flux density I_{ph}. The local specific photon consumption rate q_{ph} can be calculated by setting up a light balance over the finite layer Δz. Having calculated the average specific rate of photosynthesis, the average specific growth rate can be calculated, and from that volumetric productivity of a photobioreactor.

Volumetric productivity versus biomass concentration

In Figure 26 the volumetric productivity r_x is presented as a function of the biomass concentration C_x for a photobioreactor with a 3 cm optical path. Results are shown both for the approach based on Blackman without spectral resolution and Jassby and Platt including spectral resolution.

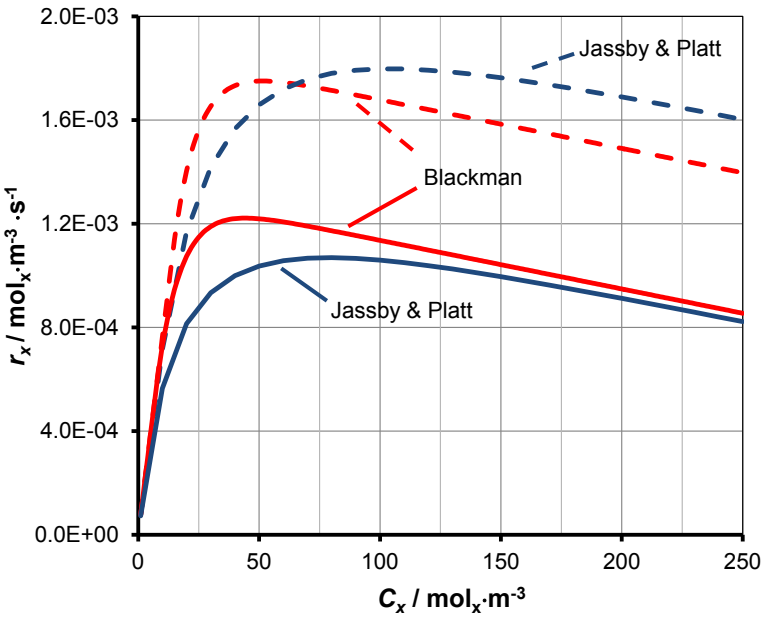

Figure 26: Volumetric productivity of a photobioreactor r_x as a function of biomass concentration C_x according to Blackman (red lines) and Jassby & Platt (blue lines). Solid lines represent results for $I_{ph}(0)$ = $0.75 \cdot 10^{-3}$ mol$_{ph}$·m^{-2}·s^{-1}, dashed lines represent results for $I_{ph}(0)$ = $1.5 \cdot 10^{-3}$ mol$_{ph}$·m^{-2}·s^{-1}. Photobioreactor: d = 0.03 m. Parameter values are based on high-light acclimated *Chlorella sorokiniana* and a sunlight spectrum: a_x = 3.33 m^2·mol$_x^{-1}$; $E_{n,\lambda}$ for sunlight; $Y^c_{s/ph,m}$ = 0.10 mol$_s$·mol$_{ph}^{-1}$; $q^c_{s,m}$ = $1.25 \cdot 10^{-4}$ mol$_s$·mol$_x^{-1}$·s^{-1}; $Y_{x/s}$ = 0.625 mol$_x$·mol$_s^{-1}$; m_s = $3.0 \cdot 10^{-6}$ mol$_s$·mol$_x^{-1}$·s^{-1}.

[2] The photic zone is defined as that part of the microalgal culture the specific rate of sugar production in the chloroplast q^c_s (i.e. photosynthesis) is higher than the maintenance requirement for sugar m_s

Both models yield different numbers but the general trend is identical. Photobioreactor productivity is highest at a certain biomass concentration which will be called the optimal biomass concentration $C_{x,opt}$. When the biomass concentration is lower than this optimal value light will pass the reactor unused. When the biomass concentration is higher than optimal the photon flux density in part of the reactor volume is below the compensation point of photosynthesis. In this part of the reactor intracellular sugar will be respired by the microalgae in order to fulfil maintenance requirements. This photosynthetically derived sugar is not available anymore for biomass growth and potential productivity is lost. This effect will be analysed in more detail below based on the Blackman model.

The results of the calculations based on Blackman without spectral resolution and Jassby and Platt approach with spectral resolution are different. This is partly related to the hyperbolic tangent function which more accurately describes the change from light-limited to light-saturated photosynthesis. The Blackman model overestimates photosynthetic rate in the transition from light limitation to light saturation (200-750 $\mu mol_{ph} \cdot m^{-2} \cdot s^{-1}$, see Figure 19). This explains the fact that at 750 $\mu mol_{ph} \cdot m^{-2} \cdot s^{-1}$ incident light productivity is higher according to Blackman (Figure 26). In addition, spectral effects are important. At a higher photon flux density of $1.5 \cdot 10^{-3}$ $mol_{ph} \cdot m^{-2} \cdot s^{-1}$ the Jassby and Platt approach results in a higher productivity (Figure 26). This approach takes into account the change of spectrum when sunlight passes through the microalgal culture. The light loses the blue and red wavelengths faster than the green wavelengths. This results in an effective decrease of the optical cross section a_x of the microalgae and a reduced level of light saturation and increased volumetric productivity.

The model calculations presented in Figure 26 were based on a high-light acclimated culture. In reality, at higher biomass concentration the microalgal culture as a whole will experience light limitation. Consequently, on a time scale of hours the microalgae will increase their pigmentation and their optical cross section (i.e. specific light absorption coefficient). The dynamics of photacclimation processes and its effect on photobioreactor productivity will be discussed later in more details but it will alter the shape of the curves presented in Figure 26 to some extent.

The existence of a point of optimal productivity can be analytically deduced employing the Blackman model without spectral resolution. The relation between volumetric productivity and biomass concentration plotted in Figure 26 is given by the following relation already introduced:

$$r_x = \frac{Y_{x/s}}{d} \cdot \left\{ \frac{q^c_{s,m}}{a_x} \cdot \left(1 + Ln\left(\frac{I_{ph}(0) \cdot a_x \cdot Y^c_{s/ph,m}}{q^c_{s,m}} \right) \right) - Y^c_{s/ph,m} \cdot I_{ph}(0) \cdot e^{-a_x \cdot C_x \cdot d} \right\} - Y_{x/s} \cdot m_s \cdot C_x$$

The function is concave meaning that the point of maximal productivity is characterized by the derivative of function $r_x = f(C_x)$ being equal to zero.

$$f'(c_x) = Y_{x/s} \cdot Y^c_{s/ph,m} \cdot a_x \cdot I_{ph}(0) \cdot e^{-a_x \cdot C_x \cdot d} - Y_{x/s} \cdot m_s$$

$$\Rightarrow 0 = Y_{x/s} \cdot Y^c_{s/ph,m} \cdot a_x \cdot I_{ph}(0) \cdot e^{-a_x \cdot C_x \cdot d} - Y_{x/s} \cdot m_s$$

$$\Leftrightarrow \frac{m_s}{Y^c_{s/ph,m} \cdot a_x} = I_{ph}(0) \cdot e^{-a_x \cdot C_x \cdot d}$$

This relation is equivalent to: $I_{ph,c} = I_{ph}(d)$

The outcome shows that at the point of maximal volumetric productivity the photon flux density at the 'backside' of the photobioreactor $I_{ph(d)}$ is equal to the compensation point of photosynthesis $I_{ph,c}$ which was derived earlier:

$$I_{ph,c} = \frac{m_s}{Y^c_{s/ph,m} \cdot a_x}$$

Given a certain photon flux density $I_{ph(0)}$ at the light-exposed surface the optimal biomass concentration $C_{x,opt}$ can now be estimated based on the Blackman approach:

$I_{ph}(d) = I_{ph,c}$ and $I_{ph}(d) = I_{ph}(0) \cdot e^{-a_x \cdot C_{x,opt} \cdot d}$

Combining these relations gives:

$$C_{x,opt} = \frac{1}{a_x \cdot d} \cdot Ln\left(\frac{I_{ph}(0)}{I_{ph,c}} \right)$$

Also when employing more realistic and more complex models, such as Jassby & Platt with spectral resolution the same rule applies: "*volumetric productivity of a photobioreactor is maximal when the biomass density is such that the photon flux density at the darkest zone of the reactor is equal to the compensation point of photoautotrophic growth*." In practice it has also been confirmed that photobioreactors can be operated at maximal productivity when the biomass concentration is maintained at those levels that almost all light is absorbed within the microalgal culture but at the back still a minimal amount of light is left to compensate for maintenance purposes (Takache et al. 2012; Barbera et al. 2015; Zijffers et al. 2010).

Volumetric productivity and biomass yield on photons versus photon flux density

Another interesting aspect about photobioreactor performance is the relation between volumetric productivity r_x and incident photon flux density $I_{ph}(0)$. Both the Blackman model without spectral resolution and the Jassby and Platt model with spectral resolution can be used to quantify this relation. The result is shown in Figure 27. At all photon flux densities simulated the optimal biomass concentration was used, which needed to be calculated first. The volumetric productivity increases with increasing incident photon flux density and, consequently, light is limiting growth even at high photon flux density. The increase, however, is not linear and the rate of increase slowly levels off. This is a consequence of increased light saturation close to the reactor surface where light levels are far above the saturating photon flux density.

This trend of r_x versus $I_{ph}(0)$ can be better understood by calculating the efficiency of light use and thus calculating the biomass yield on photons $Y_{x/ph}$. For this we need the specific photon consumption rate q_{ph}. The q_{ph} can be estimated from the light balance over the photobioreactor if we assume that all the light incident on the reactor surface is absorbed by the microalgal biomass inside the reactor. This results in the following relation:

$$-q_{ph} = \frac{I_{ph}(0) \cdot A_{r,light}}{V_r \cdot C_{x,opt}} \qquad [\mathrm{mol_{ph} \cdot mol_x^{-1} \cdot s^{-1}}]$$

The word ‘estimated’ is used because at the back of the reactor a small amount of light will leave the system since $I_{ph}(d) = I_{ph,c} > 0$. This light in fact is not useful since it is less than needed to compensate for maintenance. The biomass yield on photons $Y_{x/ph}$ then can be calculated as follows:

$$Y_{x/ph} = \frac{\overline{\mu}}{-q_{ph}} \qquad [\mathrm{mol_x \cdot mol_{ph}^{-1}}]$$

The result of this calculation is presented as well in Figure 27. The biomass yield on photons is maximal at a photon flux density of about $400 \cdot 10^{-6}$ mol·m^{-2}·s^{-1} in this example. Above this light level the yield continuously decreases with increasing $I_{ph}(0)$ because of light saturation. At photon flux density lower than $400 \cdot 10^{-6}$ mol·m^{-2}·s^{-1} the yield decreases because of the fact that an increasing part of the light absorbed is used for maintenance purposes and not for growth.

Clearly, light is used most efficiently when the photon flux density at the reactor surface is not too high, and not too low. A light level of $400 \cdot 10^{-6}$ mol·m^{-2}·s^{-1} appears to be optimal for the example illustrated in Figure 27 which is based on the green microalgae *Chlorella sorokiniana* with a high maximal specific

growth rate. Moreover it is assumed that this microalga is high-light acclimated. According to the more accurate Jassby and Platt approach a maximal biomass yield of 0.045 $mol_x \cdot mol_{ph}^{-1}$ can be expected. This can be recalculated to 1.08 $g \cdot mol_{ph}^{-1}$ assuming a biomass molar weight of 24 $g \cdot mol_x^{-1}$. In lab-scale experiments yields as high as 1.25 $g \cdot mol_{ph}^{-1}$ have been measured (Cuaresma et al. 2011), which might be related to the relatively high estimate of the maintenance requirement in the model calculations. In case the maintenance is reduced from 3.0 to $1.0 \cdot 10^{-6}$ $mol_s \cdot mol_x \cdot s^{-1}$ a yield of 1.24 $g \cdot mol_{ph}^{-1}$ can be simulated.

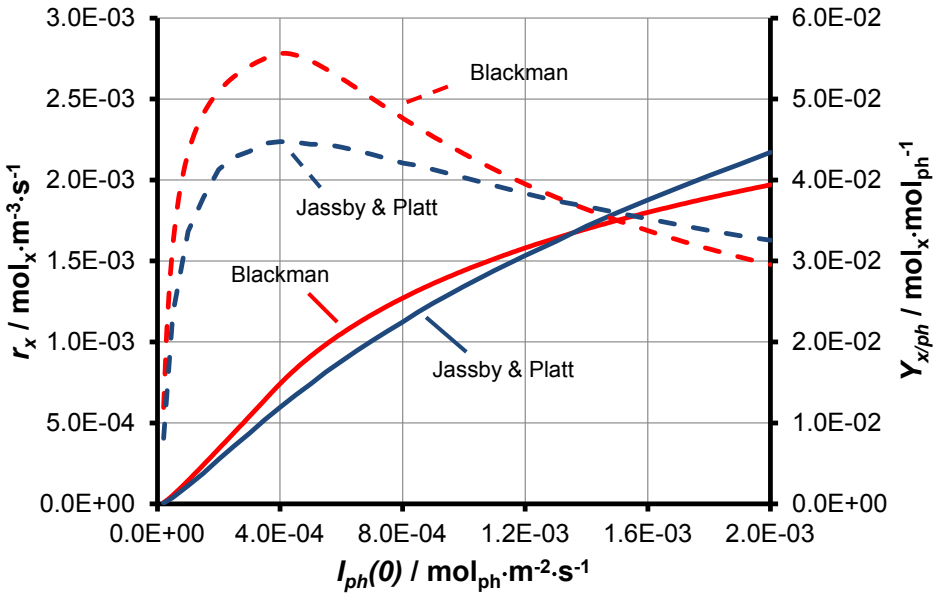

Figure 27: Volumetric productivity of a photobioreactor r_x as a function of photon flux density $I_{ph}(0)$ at the point of maximal productivity ($C_x = C_{x,opt}$) according to Blackman (solid red line) and Jassby & Platt (solid blue line). In addition, biomass yield on photons $Y_{x/ph}$ is shown as a function of $I_{ph}(0)$ according to Blackman (dashed red line) and Jassby & Platt (dashed blue line). Photobioreactor: d = 0.03 m. Parameter values are based on high-light acclimated *Chlorella sorokiniana* and a sunlight spectrum: a_x = 3.33 $m^2 \cdot mol_x^{-1}$; $E_{n,\lambda}$ for sunlight; $Y^c_{s/ph,m}$ = 0.10 $mol_s \cdot mol_{ph}^{-1}$; $q^c_{s,m}$ = $1.25 \cdot 10^{-4}$ $mol_s \cdot mol_x^{-1} \cdot s^{-1}$; $Y_{x/s}$ = 0.625 $mol_x \cdot mol_s^{-1}$; m_s = $3.0 \cdot 10^{-6}$ $mol_s \cdot mol_x^{-1} \cdot s^{-1}$.

The two different model approaches, Blackman without spectral resolution and Jassby and Platt with spectral resolution, again lead to different results (Figure 27). This aspect was already covered when discussing the results presented in Figure 26. The Blackman model overestimates the photosynthetic rate in the transition from light limitation to light saturation leading to a higher volumetric productivity and biomass yield on photons. Only at photon flux density above $1.4 \cdot 10^{-3}$ $mol \cdot m^{-2} \cdot s^{-1}$ the Jassby and Platt approach results in higher productivity and biomass yield on photons. This is related to the

incorporation of the spectral differences of specific light absorption. This results in an effective decrease of the optical cross section a_x of the microalgae and a reduced level of light saturation when light travels through the microalgal culture. This effect becomes dominant only at high photon flux density.

3.3 Microalgal cultivation in photobioreactors: photobioreactor operation

Microalgae can be grown batch wise in photobioreactors. In case biomass concentrations become too high the culture is diluted, and biomass is harvested, after which growth is allowed to continue again. Microalgae production systems can also be operated in a continuous manner based on a chemostat or turbidostat mode of operation. Here these three different operation modes will be shortly addressed. The biomass balance over the photobioreactor serves as a starting point of this evaluation:

$$V_r \cdot \frac{dC_x}{dt} = F_{in} \cdot C_{x,in} - F_{out} \cdot C_{x,out} + r_x \cdot V_r$$

Batch operation

In a batch wise cultivation there is no dilution with water and nutrients and the biomass balance can be simplified to the following relation:

$$\frac{dC_x}{dt} = \bar{\mu} \cdot C_x \qquad \Rightarrow \frac{1}{C_x} \cdot dC_x = \bar{\mu} \cdot dt$$

This relation can be integrated from time *0* to *t* provided the specific growth rate is constant and not dependent on the biomass concentration. The average specific growth rate in a microalgal culture in a photobioreactor, however, is strongly dependent on the biomass concentration. This dependency is expressed in below relation which was already derived from the Blackman model.

$$\bar{\mu} = Y_{x/CH2O} \cdot \left\{ \frac{z_s}{d} \cdot q^c_{CH2O,m} + \frac{Y^c_{CH2O/ph,m} \cdot I_{ph}(0)}{d \cdot C_x} \left(e^{-a_x \cdot C_x \cdot z_s} - e^{-a_x \cdot C_x \cdot d} \right) \right\} - Y_{x/CH2O} \cdot m_{CH2O}$$

Clearly, no simple analytical solution of the differential equation derived from the biomass balance can be obtained. Adopting numerical methods based on this differential equation the increase in biomass in time in a batch culture can still be calculated. In Figure 28 batch growth is simulated based on the model of Jassby and Platt including spectral resolution. This simulation is based on *Chlorella sorokiniana* grown under a constant photon flux density of $1.5 \cdot 10^{-3}$ $mol_{ph} \cdot m^{-2} \cdot s^{-1}$. The biomass

concentration increases in time but the rate of increase slows down. This is more apparent in the yield of biomass on photons which is maximal after about 24 hours after which it decreases again. At 24 hours the biomass concentration is optimal in the sense that at this point in time the volumetric productivity, as well as the biomass yield on light, is maximal.

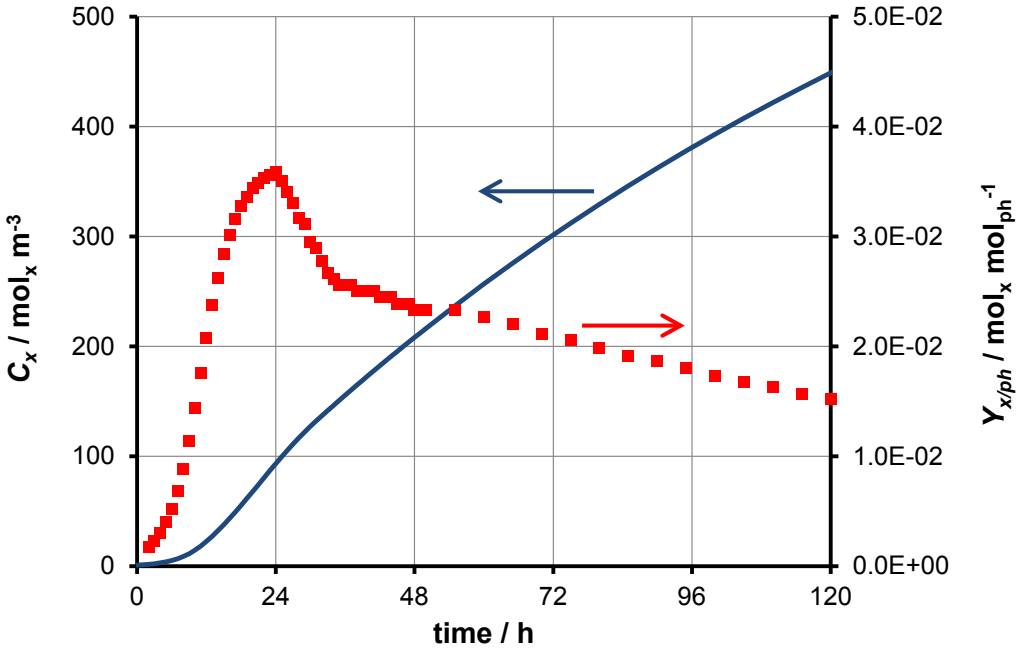

Figure 28: Simulated biomass concentration (solid blue line) and biomass yield on photons (red square markers) during batch growth of *Chlorella sorokiniana*. The biomass balance was solved based on a numerical routine taking fixed time steps of 1 minute. Simulation was based on the Jassby & Platt model including spectral resolution. Photobioreactor: d = 0.03 m; $I_{ph}(0)$ = $1.5 \cdot 10^{-3}$ $mol_{ph} \cdot m^{-2} \cdot s^{-1}$. Parameter values: a_x = 3.33 $m^2 \cdot mol_x^{-1}$; $E_{n,\lambda}$ for sunlight; $Y^c_{s/ph,m}$ = 0.10 $mol_s \cdot mol_{ph}^{-1}$; $q^c_{s,m}$ = $1.25 \cdot 10^{-4}$ $mol_s \cdot mol_x^{-1} \cdot s^{-1}$; $Y_{x/s}$ = 0.625 $mol_x \cdot mol_s^{-1}$; m_s = $3.0 \cdot 10^{-6}$ $mol_s \cdot mol_x^{-1} \cdot s^{-1}$. Photoacclimation was simulated in an arbitrary manner: after having reached the maximal productivity after 24 hours it was assumed that the specific light absorption coefficient a_x decreased linearly in time from the minimal level of 3.33 $m^2 \cdot mol_x^{-1}$ to a maximal level of 6.66 $m^2 \cdot mol_x^{-1}$ in a period of 10 hours.

The effect of photoacclimation is included in an arbitrary manner in this simulation (Figure 28). After having reached the maximal productivity after 24 hours it was assumed that the optical cross section a_x decreased linearly in time from its minimal level to its maximal level in a period of 10 hours. Such timeframe is in accordance with recent results obtained for *Chlorella sorokiniana* in the Bioprocess Engineering group of Wageningen University and an example will be given alter in this chapter. This simulated process of photoacclimation results in a rapid decline of the biomass yield on light and thus photobioreactor volumetric productivity in the 10 hour period after having reached the maximal

productivity. This trend is confirmed by published work of the same group (Kliphuis, Janssen, et al. 2011) in which clear peaks in the oxygen and carbon dioxide exchange rates were observed during batch growth in a photobioreactor. This trend also confirms the expectation that low pigmented microalgae yield higher photobioreactor productivity and higher biomass yield on light (Formighieri et al. 2012; Sukenik et al. 1987).

When operating photobioreactors or raceway ponds in batch mode a compromise must be found between achieving a high volumetric productivity (i.e. high biomass yield on light), or a high biomass concentration. A high biomass concentration results in reduced costs for processing of the microalgal suspension as less water needs to be removed and treated. A high volumetric productivity of the photobioreactor guarantees efficient use of money invested in the production system. Models describing microalgal growth as a function of microalgal biomass concentration as here discussed must be used to select the most economical and/or most sustainable operation process for photobioreactors.

Chemostat and turbidostat operation under continuous light

Microalgae can also be grown continuously meaning that the microalgal culture is continuously harvested and the liquid volume removed is continuously replaced with fresh water with nutrients. In the case of chemostat operation the dilution rate is fixed. Assuming a constant photon flux density a steady state will be reached where the biomass concentration does not change anymore and is constant. The influent, water with nutrients, usually does not contain any microalgae. Furthermore, the liquid volume is usually maintained constant, so: $F_{in} = F_{out} = F$. Finally, it will be assumed that the liquid inside the photobioreactor is perfectly mixed, so: $C_{x,out} = C_x$. Then the biomass balance over the photobioreactor can be simplified as follows:

$$F \cdot C_x = \bar{\mu} \cdot C_x \cdot V_r$$

$$\Leftrightarrow F = \bar{\mu} \cdot V_r$$

$$\Leftrightarrow \bar{\mu} = \frac{F}{V_r} = D \qquad [s^{-1}]$$

The parameter D is the dilution rate with unit s^{-1}. The inverse of the dilution rate is the hydraulic retention time HRT of the liquid inside the photobioreactor with unit s. It is the average residence time of the liquid and microalgae inside the photobioreactor.

$$\Leftrightarrow \frac{1}{D} = \frac{V_r}{F} = HRT \qquad [s]$$

When operating a photobioreactor as a chemostat the dilution rate is fixed and the microalgae are forced to grow with a specific growth rate equalling the dilution rate. The optimal dilution rate can be selected based on the relations derived before coupling the average specific growth and the biomass concentration in a photobioreactor. Please note that the product of biomass concentration and specific growth rate gives the volumetric productivity of the photobioreactor. Also in case of chemostat operation a balance needs to be found between achieving a high volumetric productivity of the photobioreactor and a high biomass concentration in the outflow.

A turbidostat mode of operation relies on the use of a sensor to measure the biomass concentration in the photobioreactor. Such a sensor can be based on the online measurement of culture turbidity, for example, but any other biomass sensor can be used as well. Based on such a continuous biomass measurement the flow rate through the system then is automatically adjusted such that the biomass concentration is maintained at a pre-selected value (Figure 29).

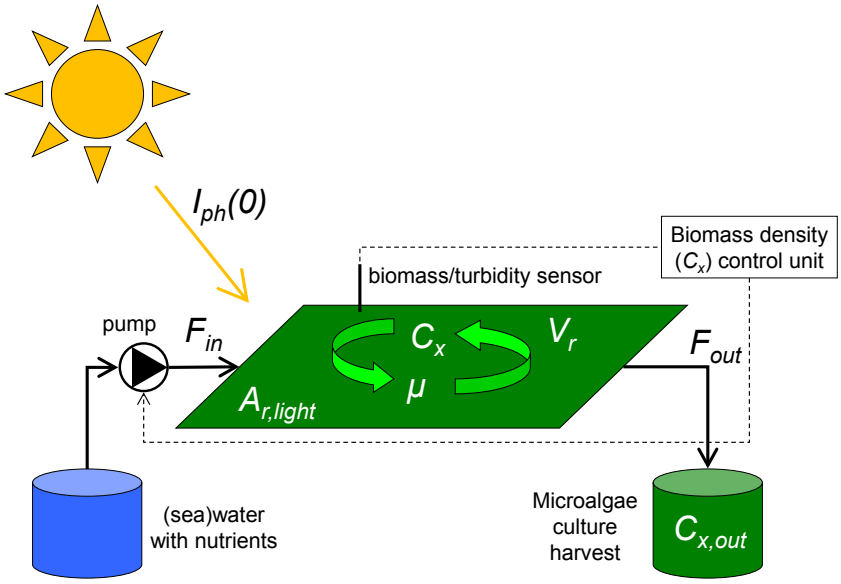

Figure 29: Schematic of turbidostat mode of operation of a microalgae cultivation system

The biomass balance over the photobioreactor then results in the same relation as the one derived for the chemostat:

$$\bar{\mu} = \frac{F}{V_r} = D$$

What happens is that the biomass concentration is fixed and determines the light gradient in the system. The local photon flux density then determines the local specific rates of photosynthesis resulting in an average specific growth rate when photosynthesis is integrated over the whole reactor volume. The biomass concentration thus determines the average specific growth rate and the turbidostat control forces the dilution rate *D* to be become equal to the specific growth rate. The advantage of a turbidostat control is that the biomass concentration can be set, and maintained, at a preferred value. The actual setting for the biomass concentration can be selected based on the relations already deduced coupling the average specific growth rate and the biomass concentration in a photobioreactor.

Chemostat and turbidostat operation under day/night cycles

Under outdoor conditions under day/night cycles biomass accumulation inside the photobioreactor cannot be neglected. Especially in case of chemostat operation considerable changes in biomass concentration will occur. Even in a turbidostat in the night biomass concentrations will decrease because of respiration. The biomass balance then must be written as follows:

$$\frac{dC_x}{dt} = \bar{\mu} \cdot C_x - D \cdot C_x$$

This differential equation can be solved numerically to analyse the performance of chemostat or turbidostat cultures under day/night cycles and results are shown in Figure 30. The average specific growth rate is calculated based on the integration of local photosynthetic rates employing the Jassby and Platt model for photosynthesis and the Lambert-Beer model for light penetration including the spectral distribution of sunlight and light absorption. It must be emphasized that this modelling approach is not optimized yet for microalgal growth under day/night cycles as it does not include the storage of carbohydrates (starch) during daytime and their use during the night. In the night microalgal growth can continue growth based on the use of these carbohydrate reserves. More specifically, microalgae synchronize their cell cycle with the day/night cycle and cell division takes place at the end of the day, or the beginning of the night (Vítová et al. 2015). In the simplified modelling approach introduced in this chapter it is assumed that all sugar produced in photosynthesis is immediately used in the light, thus in daytime. In the night only maintenance based sugar consumption is included. In

reality part of the growth-related sugar consumption is taking place in the night as these sugars are stored as starch during the day. The simulations shown in Figure 30 therefore overestimate biomass growth during the day period to some extent, but biomass loss in the night is underestimated. Both effects are assumed to cancel out over the whole day/night period.

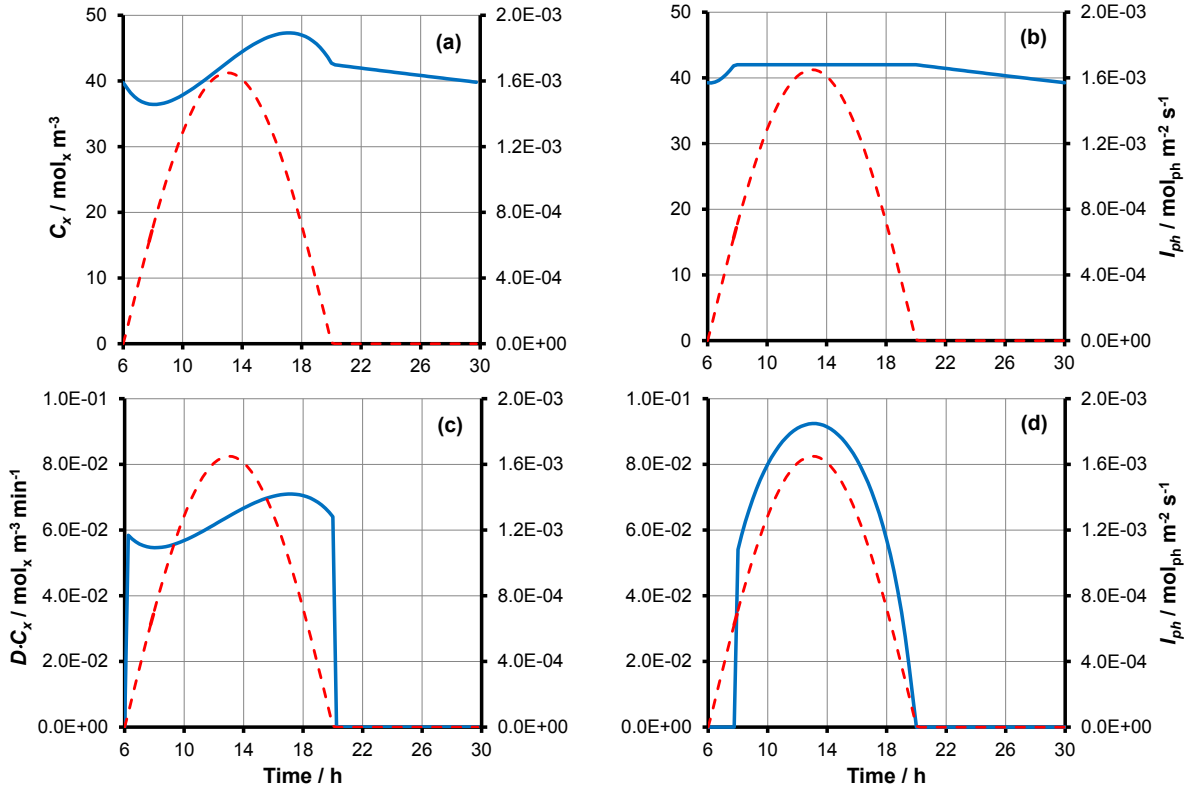

Figure 30: Simulations of chemostat (a and c) and turbidostat (b and d) operation under day/night cycles for the production of *Chlorella sorokiniana*. In upper graphs (a and b) the biomass concentration C_x is shown (solid blue lines), and in the lower graphs (c and d) the reactor productivity is shown (solid bleu lines) expressed as $D \cdot C_x$. In all graphs the photon flux density is shown as a reference (dashed red lines). Light during the day was simulated with a sine curve representing a clear-sky summer day: $I_{ph,max}$ = 1.65·10^{-3} mol$_{ph}$·m^{-2}·s^{-1}; t_{day} = 14 h. The biomass balance was solved based on a numerical routine taking fixed time steps of 1 minute. Simulation was based on the Jassby & Platt model including spectral resolution. The optical path in Lambert-Beer equation was corrected with a factor 1.5 to simulate the effect of non-perpendicular light entry along the day, and the effect of light scattering. Photobioreactor: d = 0.03 m. Setpoint chemostat: D = 0.09 h^{-1} (day period only). Setpoint turbidostat: C_x = 42 mol$_x$·m^{-3} (day period only). Parameter values: a_x = 3.33 m^2·mol$_x^{-1}$; $E_{n,\lambda}$ for sunlight; $Y^c_{s/ph,m}$ = 0.10 mol$_s$·mol$_{ph}^{-1}$; $q^c_{s,m}$ = 1.25·10^{-4} mol$_s$·mol$_x^{-1}$·s^{-1}; $Y_{x/s}$ = 0.625 mol$_x$·mol$_s^{-1}$; m_s = 3.0·10^{-6} mol$_s$·mol$_x^{-1}$·s^{-1}.

For both the chemostat and turbidostat simulations the photobioreactor was not diluted during the night. In the chemostat and turbidostat culture the biomass concentration decreases in the night due to maintenance losses. During the day in the chemostat culture the biomass concentration first

decreases to a minimal level of 36.4 $mol_x \cdot m^{-3}$ because the rate of dilution is higher than the specific growth rate at these low light levels. When the photon flux density increases growth catches up and the biomass concentration increases to a maximum of 47.3 $mol_x \cdot m^{-3}$. Only at the end of the afternoon the biomass concentration decreases again due to decreasing sunlight levels. In the turbidostat culture the biomass concentration remains constant throughout the day period. The biomass harvested from the chemostat ($D \cdot C_x$, unit $molx \cdot m^{-3} \cdot s^{-1}$) varies together with the biomass concentration. In the turbidostat the harvest is even more variable since the harvest directly follows the dilution rate which depends on the specific growth rate which is dictated again by the sunlight intensity.

Photoacclimation and a change in microalgal optical cross section was not included in these simulations. In these examples the biomass concentrations were relatively low (42 $mol_x \cdot m^{-3}$ = 1.0 $g \cdot L^{-1}$) for a photobioreactor with a 3 cm optical path. It was therefore assumed that the microalgae were high-light acclimated. The overall daily productivity simulated under these conditions was 39 $g \cdot m^{-2} \cdot d^{-1}$ for both operational strategies corresponding to a biomass yield on light ($Y_{x/ph}$) of 0.74 $g \cdot mol^{-1}$. These values correspond well to data obtained for *Chlorella sorokiniana* under similar conditions in laboratory scale experiments (Cuaresma et al. 2011; Zijffers et al. 2010).

Despite the fact that productivity of chemostat operation is similar to turbidostat operation the turbidostat is preferred especially at locations with more day-to-day variation in irradiance. Under chemostat operation biomass concentration will slowly decrease on consecutive days with cloud cover. If followed by a clear-sky day the culture is vulnerable to photoinhibition because of its low biomass concentration. Turbidostat operation allows for a direct control of biomass concentration. Wash-out of a microalage culture in a turbidostat is by definition not possible. In a chemostat this could occur in situations the dilution rate is not adjusted in time. Turbidostat operation is thus more robust and allows for reliable automation of outdoor microalgae production (Bosma et al. 2014).

4 Improving the estimation of photobioreactor productivity

4.1 Understanding and prediction photoacclimation

Photoacclimation has already been discussed. It has been shown that microalgae can adjust their optical cross section as a response to a change in light regime. It is, however, complicated to predict this photoacclimation response. Excellent attempts have been made by several research groups (Geider et al. 1998; García-Camacho et al. 2012; Ross & Geider 2009) but these result in complex models requiring the fitting of additional model parameters. These models are defined cell specific in order to take into account cell history and they will require recalculation to metrics required on a photobioreactor level. Specifically in the situation of the diurnal change in light conditions modelling, or predicting, photoacclimation is complicated because the time scale of the change in light level is in the same order as the time scale of the photoacclimation response. As an example the change in optical cross section (i.e. specific light absorption coefficient) is shown in Figure 31 as was measured for *Chlorella sorokiniana* upon a shift from high light condition to low light conditions. Within 8 hours after the shift specific light absorption already approached that of low light acclimated microalgae.

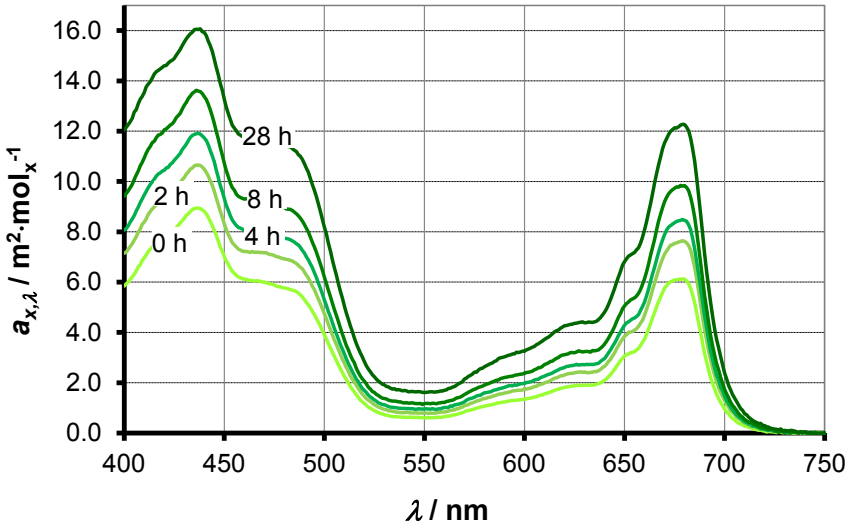

Figure 31: Dynamics of photoacclimation: change of the specific light absorption coefficient $a_{x,\lambda}$ as a response to a shift from high light to low light. The example given is based on the green microalga *Chlorella sorokiniana*. The microalgae were grown in a 14 mm plat type photobioreactor in turbidostat mode with ingoing photon flux density of $980 \cdot 10^{-6}$ $mol_{ph} \cdot m^{-2} \cdot s^{-1}$ and an outgoing photon flux density of $430 \cdot 10^{-6}$ $mol_{ph} \cdot m^{-2} \cdot s^{-1}$. At t = 0 h the ingoing photon flux density was decreased step-wise to $60 \cdot 10^{-6}$ $mol_{ph} \cdot m^{-2} \cdot s^{-1}$ and the specific absorption coefficient was measured after 2, 4, 8, and 28 hours.

Although it is challenging to incorporate photoacclimation in photobioreactor production models it is important for future improvement of microalgae production strategies. The size of the optical cross section (i.e. the specific light absorption coefficient) determines specific light absorption and the specific rate of photosynthesis. As such, also the specific growth rate and the light use efficiency strongly depend on the specific light absorption coefficient of the microalgae. This is exemplified for the green microalga *Chlorella sorokiniana* in Figure 32. Cells with a large specific light absorption coefficient are photo-saturated at lower photon flux density and express a lower biomass yield on photons at high photon flux density when compared to cells with small absorption coefficient. In Figure 32 trends are shown for high light acclimated cells (7.0 $m^2 \cdot mol_x^{-1}$) and low light acclimated cells (3.5 $m^2 \cdot mol_x^{-1}$). In addition, a model prediction is included reflecting a hypothetical mutant strain with a reduced antenna size (a_x = 1.75 $m^2 \cdot mol_x^{-1}$). Specifically the latter 'strain' is interesting because it only reaches its maximal specific growth rate at $1.5 \cdot 10^{-3}$ $mol_{ph} \cdot m^{-2} \cdot s^{-1}$ and still expresses a good biomass yield on photons (≈ 50% of maximal yield).

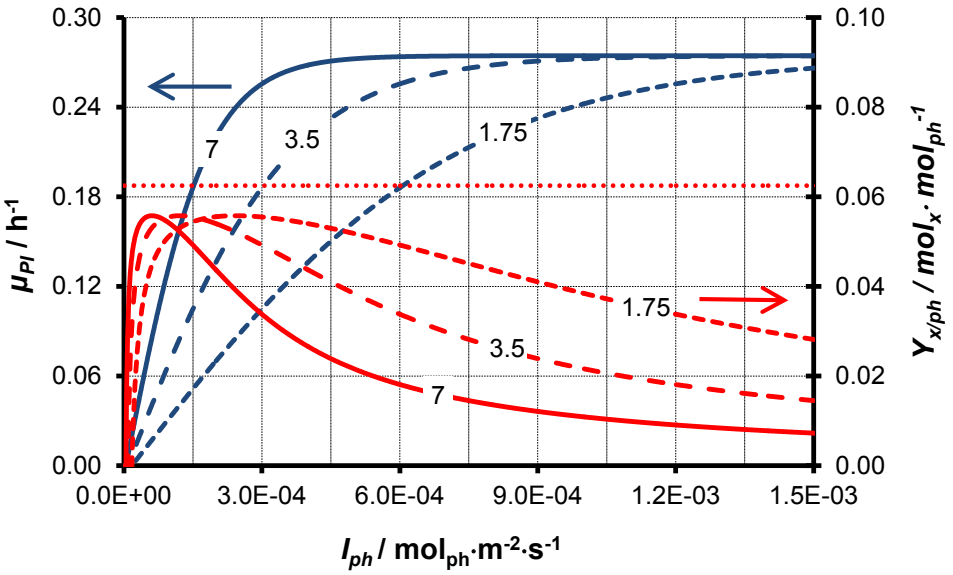

Figure 32: Instantaneous specific growth rate μ_{PI} and biomass yield on photons $Y_{x/ph}$ as a function of photon flux density I_{ph} for different values of the specific light absorption coefficient a_x. The model of Jassby & Platt was used and spectral effects were neglected, thus assuming a constant a_x. The dotted red line represents the hypothetical maximal biomass yield on photons $Y_{x/ph,m}$ (m_s = 0). Parameter values based on *Chlorella sorokiniana*: $Y^c_{s/ph,m}$ = 0.10 $mol_s \cdot mol_{ph}^{-1}$; $q^c_{s,m}$ = $1.25 \cdot 10^{-4}$ $mol_s \cdot mol_x^{-1} \cdot s^{-1}$; $Y_{x/s}$ = 0.625 $mol_x \cdot mol_s^{-1}$; m_s = $3.0 \cdot 10^{-6}$ $mol_s \cdot mol_x^{-1} \cdot s^{-1}$; M_x = 24 $g \cdot mol_x^{-1}$. Values of a_x given in figure: 7.0 $m^2 \cdot mol_x^{-1}$ (low light acclimated); 3.5 $m^2 \cdot mol_x^{-1}$ (high light acclimated); 1.75 $m^2 \cdot mol_x^{-1}$ (hypothetical antenna size mutant).

The area in Figure 32 enclosed by the curve of $Y_{x/ph}$ versus I_{ph} and the x-axis ($Y_{x/ph}$ = 0) represents the areal productivity of a photobioreactor P_x:

$$P_x = \int_{I_{ph(0)}}^{I_{ph(d)}} Y_{x/ph} \cdot dI_{ph} \qquad [mol_x \cdot m^{-2} \cdot s^{-1}]$$

This is illustrated in more detail in Figure 33. The point on the x-axis where the $Y_{x/ph}$ trend crosses ($Y_{x/ph}$ = 0) represents the compensation point of photosynthesis $I_{ph,c}$ and this would be the optimal photon flux density at the backside of a photobioreactor with a depth *d; $I_{ph}(d)$*. On the right hand side the area is not enclosed. In this specific example the x-axis runs until $1500 \cdot 10^{-6}$ $mol_{ph} \cdot m^{-2} \cdot s^{-1}$. Taking the area up to this photon flux density would mean assuming the photobioreactor to be exposed to an ingoing photon flux density of $1.5 \cdot 10^{-3}$ $mol_{ph} \cdot m^{-2} \cdot s^{-1}$; *$I_{ph}(0)$*. This analysis only holds for flat systems and neglects spectral effects with respect to light absorption. Nevertheless comparing these surfaces underneath the $Y_{x/ph}$ curves for different values of the specific light absorption coefficient (Figure 32) shows the potential effect of reduced antenna size on photobioreactor productivity. Productivity could be more than doubled when the antenna size of the photosystems is reduced with a factor 4 in comparison to the low-light acclimated microalgae.

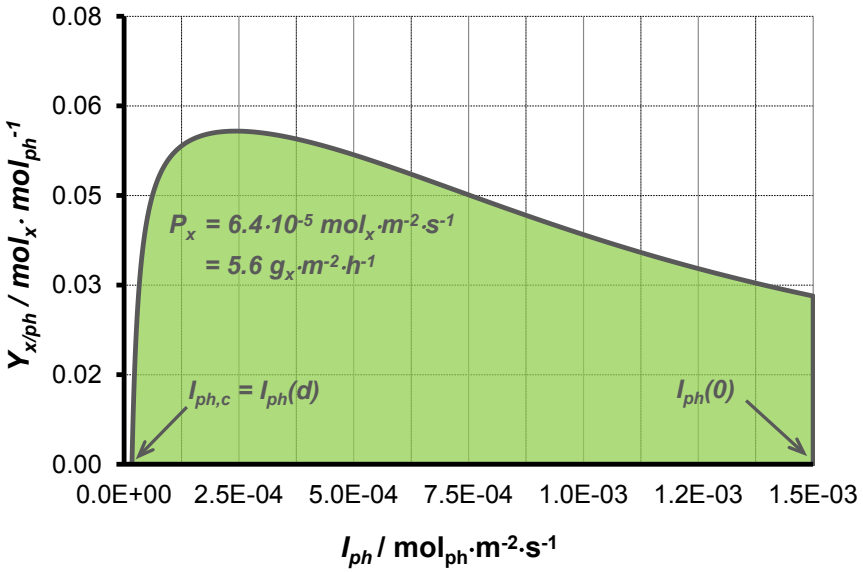

Figure 33: Illustration of the graphical estimation of photobioreactor productivity expressed per m^2 of illuminated surface. Graph is based on hypothetical antenna size mutant with a_x = 1.75 $m^2 \cdot mol_x^{-1}$. See figure 32 for more details.

Antenna size reduction unfortunately is not trivial and current antenna size mutants of *Chlamydomonas reinhardtii* for example were not able to outperform the wild type (Mooij et al. 2014).

It is important to stress that only light absorption should be reduced and that the capacity to process photons and perform photosynthesis should remain unaltered. In other words, the number of photosystems must remain maximal and only the size of the antenna complex of the photosystems should be reduced (Formighieri et al. 2012; Wobbe & Remacle 2014).

4.2 Mixing-induced light/dark cycles in photobioreactors

In the simplified model approach to predict photobioreactor productivity adopted in this chapter it was assumed that microalgae immediately respond to the local photon flux density. It was assumed that the specific rate of photosynthesis at any point in time and space is only dependent on the actual photon flux density at that point in time, and at that position within the photobioreactor. Of course this is a simplification of reality and its implications will be qualitatively discussed here.

Mixing of the microalgal suspension in photobioreactors results in a movement of individual microalgal cells over the light gradient resulting in light/dark cycles. The timescale of these events depend on reactor design and reactor operation. An evaluation of studies based on CFD modelling show that for typical photobioreactors shapes (tubes, plates, and columns) the average cycle time is in the order of seconds (Gómez-Pérez et al. 2015; Moberg et al. 2011; Olivieri et al. 2015). Only when including static mixers, or very short optical paths in combination with high liquid velocities, light/dark cycles between 0.1 and 1 s can be obtained (Moberg et al. 2011; Perner-Nochta & Posten 2007; Zhang et al. 2012). This type of mixing over the light gradient of a microalgal culture in a photobioreactor could affect photosynthesis.

<u>The flashing light effect - light dilution</u>

On a very short time scale it is hypothesised that microalgae can store the reducing power liberated during photosynthesis within the electron carriers associated to the photosynthetic electron transport chain (Vejrazka et al. 2011): plastoquinone, cytochrome, plastocyanin, ferredoxin, NADP (nicotinamide adenine dinucleotide phosphate). In addition, power can be stored by means of the electro-chemical proton gradient generated over the thylakoid membranes. The capacity of this battery will only suffice to 'store' high light flashes in the order of $1.0 \cdot 10^{-3}$ $mol_{ph} \cdot m^{-2} \cdot s^{-1}$ for about a millisecond (Vejrazka et al. 2015). In a following dark period, which is in the order of 10 milliseconds, the reducing power then can be used. The consequence of this storage effect is that high light flashes still can be used at high

photosynthetic efficiency and this is also referred to as the 'flashing light' effect (Phillips & Myers 1954). In theory this effect could be exploited by rapid mixing of microalgal suspensions in photobioreactors such that microalgae are only exposed shortly to high light at the photobioreactor surface and have sufficient time in the darker zones to process the power stored. In other words, oversaturating light at the reactor surface can be 'diluted' over the whole reactor volume. However, considering the short timescales of the flashing light effect (< 10 ms), the flashing light effect cannot be exploited in large-scale photobioreactors which have mixing times in the order of seconds.

Nevertheless, there are reports that increased and more systematic mixing enhances photobioreactor productivity (Qiang & Richmond 1996; Degen et al. 2001; Laws et al. 1986; Laws et al. 1983; Kong et al. 2013). These are all intensively mixed systems with an estimated mixing time along the light gradient in the order of a second. It is attractive to attribute this to a flashing light effect but it is more likely that other effects play a role. Downstream of the photosynthetic electron transport chain other metabolites might form another storage effect. It could be hypothesized that the capacity of the photosynthetic electron transport chain is somewhat higher than the capacity of the Calvin–Benson–Bassham cycle for carbon dioxide reduction to sugar (Stitt 1986). Such an effect, however, must not be overestimated. Consensus is growing for the concept that the capacity of photosynthetic electron transport closely matches the rate of carbon dioxide reduction by means of tight control of the actual rates and the maximal capacities of both pathways (Foyer et al. 2012).

Photoinhibition and light/dark cycling

A better explanation of the observed increase in photobioreactor productivity as a result of increased and more systematic mixing is the reduction of the effect of photoinhibition. Under oversaturating light photosystems are continuously inactivated by surplus light absorbed. At the same time inactivated photosystems are continuously repaired by a dedicated pathway: the PSII repair cycle (Nixon et al. 2010). The actual fraction of photosystems inactivated depends on the photon flux density, time of light exposure, and the rate of the repair process (Campbell & Tyystjärvi 2012). Increased mixing along the light gradient will decrease the light dose received during light exposure and will thus result in less photoinactivation. At the same time more frequent visits to the darker zones of the photobioreactor will allow the repair process to re-activate the inactivated photosystems again. This effect has already been integrated in a model description of photosynthesis by Eilers and Peeters

(Eilers & Peeters 1988), the so-called three-state model. This model has been used to predict the effect of rapid light/dark fluctuations on microalgal growth (García-Camacho et al. 2012; Rubio Camacho et al. 2003; Olivieri et al. 2015). Specifically Olivieri concluded from their modelling efforts that the phenomenon of second scale light/dark cycling in combination with the PSII repair cycle could explain frequent observations that high density microalgal culture in photobioreactors do not seem to be inhibited at high photon flux density (Olivieri et al. 2015). Light/dark fluctuations in the order of seconds could thus reduce photoinhibition and this effect should be clearly distinguished form the 'flashing light effect' which is based on a millisecond potential to store reducing power within the photosynthetic electron carriers. This flashing light effect cannot be reasonably exploited in large-scale photobioreactors.

Light dissipation, photoacclimation, and light/dark cycling

In case the time scale of mixing along the light gradient (light/dark cycling) is 10 seconds or more negative effects of light/dark cycles have been reported. Specifically long dark periods have been reported to reduce the efficiency of light utilization, or photobioreactor productivity (Barbosa et al. 2003; Janssen, Janssen, et al. 2000; Takache et al. 2015). These observations might be related to the process of photoaclimation, to the activation and de-activation of dissipative pathways for excess light absorption, or to conformational changes of the photosystem antennae (i.e. state transitions).

The biomass density in combination with the optical path of the photobioreactor determines the size of dark volume in a photobioreactor. An increase in the relative size of the dark volume will induce photoacclimation and an increase of the optical cross section (Janssen, Janssen, et al. 2000; Janssen, Bresser, et al. 2000). This will result in more over-saturation and light wasting in the light volume of the photobioreactor. One could argue that in the ideal situation there is no real dark zone and that the photon flux density at the backside should be around the compensation point photobioreactors. In practice, however, photon flux density changes within the day and it will also change from day to day. For this reason it is impossible to maintain optimal conditions for each point in time. Consequently, during many hours of the day biomass density is above the optimal value resulting in a dark zone stimulating photoacclimation and an increase of the optical cross section.

Besides adapting the optical cross section which is a relatively long process, microalgae have other tools at hand to quickly adapt to changing light conditions. Within the antenna complexes of the

photosystems conformational changes can be activated to allow safe dissipation of absorbed light energy as heat in the situation the photosystems are not able to process the energy by means of photosynthesis. These dissipative processes are usually referred to as 'non-photochemical quenching'; NPQ (Müller et al. 2001; Niyogi & Truong 2013). NPQ can be activated and de-activated on a time scale of multiple seconds to minutes. In the situation NPQ is not sufficient to dissipate excess light absorbed photosystems will be photoinactivated as discussed before.

Besides safe dissipation of light in the antennae complexes the antennae complexes itself can detach from one type of photosystem (PSII) and possibly attach again to the other type of photosystems (PSI), or vice versa (Mullineaux & Emlyn-Jones 2005; Finazzi et al. 2002; Ünlü et al. 2014). This process is called 'state transitions' and allows photosynthesis to adjust the ratio of ATP production versus NADPH production by adjusting the rates of linear electron transport through PSII and PSI, yielding NADPH and ATP, and cyclic electron transport around PSI, yielding ATP only. Also state transitions can occur on a time scale of multiple seconds to minutes. State transitions and NPQ will play a role in microalgae cultivation in photobioreactors with mixing times along the light gradient of several seconds or more. These biological regulatory processes are subject of in-depth studies and it is a huge challenge to summarize these effects in simplified models which can be used to improve model predictions of photobioreactor productivity.

Based on this evaluation of the effect of mixing along the long gradient of microalgal cultures in photobioreactors the model description of photobioreactor productivity adopted in this chapter can be evaluated. In the photobioreactor production model it was assumed that the specific rate of photosynthesis is only dependent on the actual photon flux density at that point in time, and at that position within the photobioreactor. A flashing light effect based on a limited storage capacity of electrons and diluting light over time is thus excluded, and it is fully acknowledged within the model description that light/dark cycling in the order of 10 ms is not possible in large-scale outdoor photobioreactors. In addition, photoinhibition is not included in the model description meaning that it is implicitly assumed that biomass density and mixing along the light gradient are sufficiently fast to prevent significant photodamage under over saturating photon flux density.

4.3 Diurnal variations in light intensity

On longer time scales of minutes to hours other light variations can be identified: the daily increase and decrease of light intensity, and increasing or decreasing cloud cover. These changes will activate or de-activate the same regulatory mechanisms associated to the safe dissipation of excess light energy absorbed as discussed above for light/dark cycles in the ranges of seconds to minutes. In addition, regulatory mechanisms can be activated allowing for an adjustment of the ATP:NADPH ratio required by the microalgae. On a timescale of hours photoacclimation will take place which also has been discussed already. A good summary of the biological potential of phototrophic organisms to respond to changes in light level, and light quality, is provided by Foyer (Foyer et al. 2012). Preferably the most dominant among all these mechanisms are included in a model description for photobioreactor productivity. Partly such effects are already included in cell-based models such as those of Garcia-Camacho and Ross (García-Camacho et al. 2012; Ross & Geider 2009).

The diurnal change of irradiance has been included in the model description of photobioreactor productivity under day/night cycles as visualized in Figure 30. It was assumed that all sugar produced in photosynthesis is immediately used in the light, thus in daytime. In the night only maintenance based sugar consumption is included. In reality part of the growth-related sugar consumption is taking place in the night as these sugars are stored as starch during the day. Including these dynamics will introduce additional complexity to the model description of photobioreactor productivity, but again it will improve the accuracy of model predictions. Moreover it will be important to be able to predict respiratory oxygen consumption in the night as well in order to optimize the gas exchange systems of photobioreactors.

4.4 Light direction and light scattering and photobioreactor productivity

The model description of microalgal growth in photobioreactors was based on a simplified description of the light field within microalgal cultures. The Lambert-Beer law was employed while assuming a flat photobioreactor surface (flat panels, raceway ponds, sloped cascade systems). In addition it was assumed that light entrance was always perpendicular to the light exposed surface. These assumptions allowed for a relatively simple mathematical description of photobioreactor productivity. In this manner important aspects of microalgal production processes could be highlighted. An improved description of the light field, however, will make the model predictions more reliable and is a step which must be taken when describing productivity in real outdoor microalgal production systems. The two most important aspects which must be taken into account when modelling the light field are the angle of incidence at the photobioreactor surface, and the effect of light scattering by the microalgae. In relation to that also reflection and refraction events at photobioreactor surfaces must be included, as well as photobioreactor shape and orientation. These aspects will be covered in detail in other chapters of this book. Below shortly the impact of the angle of incidence and light scattering will be discussed.

The angle of incidence from direct sunlight depends on the geographical location and varies over the day and seasons. The illustration in Figure 34 exemplifies that this results in a light path (d_θ in Figure 34) which is substantially longer than the depth of the system (d in Figure 34). The actual light path determines the optimal biomass concentration as discussed before in this chapter. In an outdoor raceway pond for example the optimal biomass concentration is much lower in early morning than around solar noon. Consequently, it is almost impossible to maintain optimal conditions throughout a day. In general the biomass concentrations will be above optimal in early morning and late afternoon when the sun is low on the horizon leading to a substantial dark zone in the microalgal culture.

The daily change in light path clearly has implications for the light field within the culture and thus the local rates of photosynthesis, and this effect must be taken into account when aiming for a reliable prediction of outdoor photobioreactor productivity. For accurate predictions the photobioreactor production models must thus be resolved for every point in time during the day. In the simulations of outdoor systems presented in Figure 30 the optical path was corrected with a factor 1.5 to partly accommodate for this effect to make the predictions more in line with the outcome of real systems. A factor of 1.5 is equivalent to an angle 48° between the light ray and the normal of the surface. The real

angle of incidence of sunlight is higher due to refraction at the photobioreactor surface, which is also illustrated in Figure 34. It is interesting to note that refraction leads to spreading of collimated sunlight and thus light dilution, which will lead to less oversaturation of individual microalgal cells at the photobioreactor surface. This effect has been included in a future outlook on large-scale microalgae production by Breuer (Breuer et al. 2015). The factor 1.5 adopted for the simulation presented in Figure 30 was an arbitrary choice but it can be placed in perspective by calculating the average light path travelled by perfectly diffused (i.e. isotropic) light through a flat system. This calculation is illustrated in Figure 35 and it results in an average light path being exactly twice as large as the shortest path through the culture along the normal of the surface. This is equivalent to an average angle between light beam and surface normal of 60°.

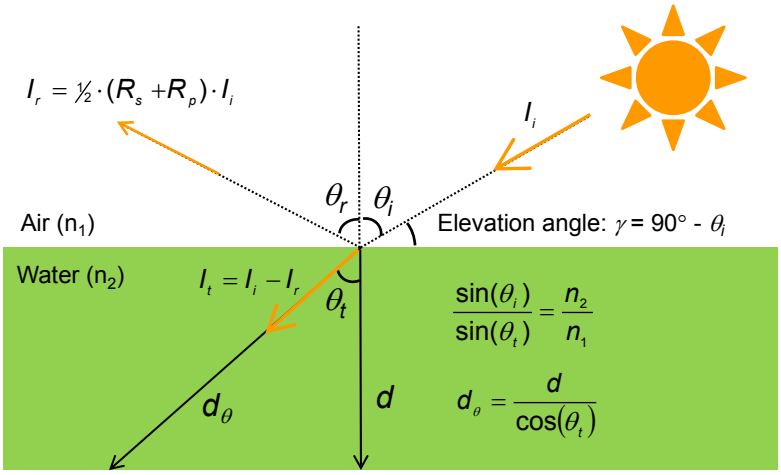

Figure 34: Illustration of the relation between angle of incidence θ_i on a photobioreactor and the light path through a microalgal culture d_θ. In this example the situation in a microalgal pond system is illustrated. In addition to light path also the effect of light refraction and reflection at the culture surface is illustrated including Snell's Law. Factors R_s and R_p must be calculated with the Fresnel equations.

In Figure 35 collimated sunlight is diffused by clouds. Clouds will reduce sunlight irradiance on ground surface and will indeed lead to less direct irradiance and a more diffuse irradiance. However, within the microalgal culture light scattering by the microalgal cells will also lead to a more isotropic character of the light field. Light scattering has been discussed before and was already illustrated in Figure 9. Also light scattering will lead to an increase of the light path in relation to culture depth *d*. On the one hand, the increase of light path can even be higher than the factor 2 derived for isotropic light (Figure 35). This is related to the fact that a light flux will develop within the culture in the opposite direction of the entry of light. On the other hand, it was observed in practice that a light path correction factor of

1.2 to 1.6 was sufficient to accommodate for this effect (unpublished data Bioprocess engineering, Wageningen University) when employing Algaemist laboratory scale photobioreactors (Mooij et al. 2014) illuminated with quasi-collimated light. Including scattering within model predictions of the light field in microalgal cultures in photobioreactors will be discussed in other chapters of this book. It is a big challenge and requires complex mathematical and numerical routines. Such an approach must also include the effect of reactor shape and orientation. An accurate description of the light field though is necessary for a more reliable description and prediction of photobioreactor productivity.

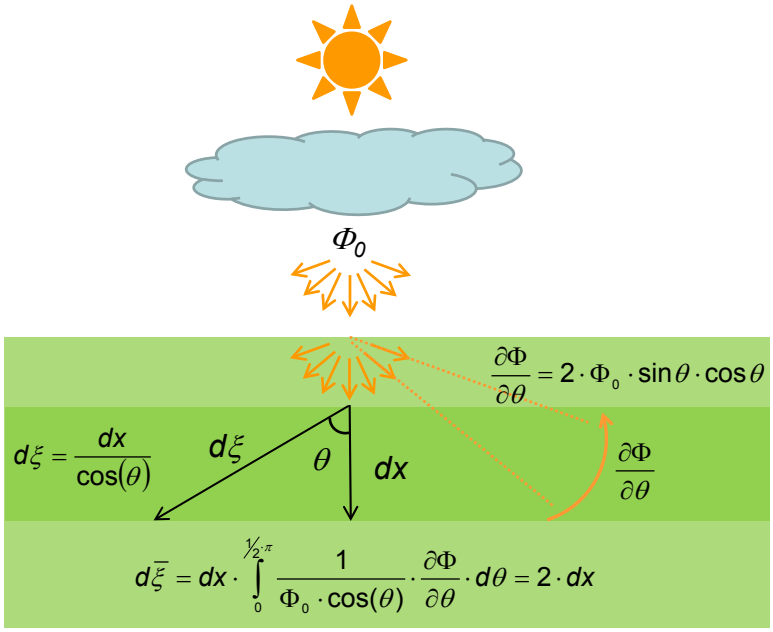

Figure 35: Diffused light and average light path through a microalgal culture. The parameter Φ represents the total radiant flux or photon flux (unit W or $mol_{ph}\cdot s^{-1}$).

5 References

Allen JF: Cyclic, pseudocyclic and noncyclic photophosphorylation: New links in the chain, Trends in Plant Science 8(1):15–19, 2003.

Barbera E, Sforza E, Bertucco A: Maximizing the production of *Scenedesmus obliquus* in photobioreactors under different irradiation regimes: experiments and modeling, Bioprocess and Biosystems Engineering, published online 20 August 2015, doi:10.1007/s00449-015-1457-9.

Barbosa MJ, Janssen M, Ham N, et al: Microalgae cultivation in air-lift reactors: modeling biomass yield and growth rate as a function of mixing frequency. Biotechnology and Bioengineering 82(2):170–9, 2003.

Björkman O, Demmig B: Photon yield of O_2 evolution and chlorophyll fluorescence characteristics at 77 K among vascular plants of diverse origins, Planta 170:489–504,1987.

Blackman FF: Optima and limiting factors, Annals of Botany 19:281–296, 1905.

Blanken W, Cuaresma M, Wijffels RH, et al: Cultivation of microalgae on artificial light comes at a cost, Algal Research 2(4):333–340, 2013.

Bosma R, de Vree JH, Slegers PM, et al: Design and construction of the microalgal pilot facility AlgaePARC, Algal Research 6:160-169, 2014.

Breuer G, Lamers PP, Janssen M, et al: Opportunities to improve the areal oil productivity of microalgae, Bioresource Technology 186:294–302, 2015.

Campbell DA, Tyystjärvi E: Parameterization of photosystem II photoinactivation and repair, Biochimica et Biophysica Acta - Bioenergetics 1817(1):258–265, 2012.

Cape JL, Bowman MK, Kramer DM: Understanding the cytochrome *bc* complexes by what they don't do. The Q-cycle at 30. Trends in Plant Science 11(1):46–55, 2006.

Chalker BE: Modelling light saturation curves for photosynthesis: an exponential function, Journal of Theoretical Biology 84:205–213, 1980.

Chen F, Johns MR: Effect of C/N ratio and aeration on the fatty acid composition of heterotrophic *Chlorella sorokiniana*, Journal of Applied Phycology 3:203–209, 1991.

Cordier J-L, Butsch BM, Birou B, et al: The relationship between elemental composition and heat of combustion of microbial biomass, Applied Microbiology and Biotechnology 25(4):305–312, 1987.

Cuaresma M, Janssen M, Vílchez C, etal: Horizontal or vertical photobioreactors? How to improve microalgae photosynthetic efficiency, Bioresource Technology 102(8):5129–37, 2011.

Davies-Colley RJ, Pridmore RD, Hewitt JE: Optical properties of some freshwater phytoplanktonic algae, Hydrobiologia 133(2):165–178, 1986.

Degen J, Uebele A, Retze A, et al: A novel airlift photobioreactor with baffles for improved light utilization through the flashing light effect, Journal of Biotechnology 92:89–94, 2001.

Dubinsky Z, Falkowski PG, Wyman K: Light harvesting and utilization by phytoplankton, Plant and Cell Physiology 27(7):1335–1349, 1986.

Dubinsky Z, Stambler N: Photoacclimation processes in phytoplankton: mechanisms, consequences, and applications, Aquatic Microbial Ecology, 56(September):163–176, 2009.

Eilers PHC, Peeters JCH: A model for the relationship between light intensity and the rate of photosynthesis in phytoplankton, Ecological Modelling, 42:199–215, 1988.

Emerson R, Lewis CM: The dependence of the quantum yield of *Chlorella* photosynthesis on wavelength of Light. American Journal of Botany 30(3):165-178, 1943.

Evans J: The dependence of quantum yield on wavelength and growth irradiance, Australian Journal of Plant Physiology 14:69-79, 1987.

Finazzi G, Rappaport F, Furia A, et al: Involvement of state transitions in the switch between linear and cyclic electron flow in *Chlamydomonas reinhardtii*, EMBO Reports 3(3):280–285, 2002.

Formighieri C, Franck F, Bassi R: Regulation of the pigment optical density of an algal cell: Filling the gap between photosynthetic productivity in the laboratory and in mass culture, Journal of Biotechnology, 162(1):115–123, 2012.

Foyer CH, Neukermans J, Queval G, et al: Photosynthetic control of electron transport and the regulation of gene expression, Journal of Experimental Botany 63(4):1637–1661, 2012.

García-Camacho F, Sánchez-Mirón A, Molina-Grima E, et al: A mechanistic model of photosynthesis in microalgae including photoacclimation dynamics, Journal of Theoretical Biology 304:1–15, 2012.

Geider RJ, MacIntyre HL, Kana TM: A dynamic regulatory model of phytoplanktonic acclimation to light, nutrients, and temperature, Limnology and Oceanography 43(4):679–694, 1998.

Geider RJ, Osborne BA: Respiration and microalgal growth: a review of the quantitative relationship between dark respiration and growth, New Phytologist 112(3):327–341, 1989.

Gómez-Pérez CA, Espinosa J, Montenegro Ruiz LC, et al: CFD simulation for reduced energy costs in tubular photobioreactors using wall turbulence promoters, Algal Research, 12:1–9, 2015.

Heijnen JJ, Van Dijken JP: In search of a thermodynamic description of biomass yields for the chemotropic growth of microorganisms, Biotechnology and Bioengineering 42(9):833-858, 1992.

Heijnen SJ: Thermodynamics of microbial growth and its implications for process design, Trends in Biotechnology 12(12):483-492, 1994.

Hogewoning SW, Wientjes E, Douwstra P, et al: Photosynthetic Quantum Yield Dynamics: From Photosystems to Leaves, The Plant Cell 24(5):1921–1935, 2012.

Janssen M, Janssen M, de Winter M, et al: Efficiency of light utilization of *Chlamydomonas reinhardtii* under medium-duration light/dark cycles, Journal of Biotechnology, 78(2), 123–137, 2000a.

Janssen M, de Bresser L, Baijens T, et al. Scale-up aspects of photobioreactors : effects of mixing-induced light / dark cycles, Journal of Applied Phycology 12:225–237, 2000b.

Jassby AD, Platt T: Mathematical formulation of the relationship between photosynthesis and light for phytoplankton. Limnology and Oceanography 21(4):540-547, 1976.

Kirk JTO: Light and photosynthesis in aquatic ecosystems (second edition), 1994, Cambridge University Press.

Kliphuis AMJ, de Winter L, Vejrazka C, et al: Photosynthetic efficiency of *Chlorella sorokiniana* in a turbulently mixed short light-path photobioreactor, Biotechnology Progress 26(3):687–696, 2010.

Kliphuis AMJ, Janssen M, van den End EJ, et al: Light respiration in *Chlorella sorokiniana*, Journal of Applied Phycology 23(6):935–947, 2011.

Kliphuis AMJ, Klok AJ, Martens DE, et al: Metabolic modeling of *Chlamydomonas reinhardtii*: Energy requirements for photoautotrophic growth and maintenance, Journal of Applied Phycology 24(2):253–266, 2012.

Kliphuis AMJ, Martens DE, Janssen M, et al: Effect of O_2:CO_2 ratio on the primary metabolism of *Chlamydomonas reinhardtii*. Biotechnology and Bioengineering, 108(10):2390–402, 2011.

Kong B, Shanks JV, Vigil RD: Enhanced algal growth rate in a Taylor vortex reactor, Biotechnology and Bioengineering 110(8):2140–2149, 2013.

Kramer DM, Evans JR: The importance of energy balance in improving photosynthetic productivity, Plant Physiology, 155(1):70–78, 2011.

Laws EA, Taguchi S, Hirata J, et al: High algal production rates achieved in a shallow outdoor flume, Biotechnology and Bioengineering 28(698):191–197, 1986.

Laws EA, Terry KL, Wickman J, et al: A simple algal production system designed to utilize the flashing light effect, Biotechnology and Bioengineering 25:2319–2335, 1983.

Lee Y-K, Ding S-Y, Hoe C-H, et al: Mixotrophic growth of *Chlorella sorokiniana* in outdoor enclosed photobioreactor, Journal of Applied Phycology 8:163–169, 1996.

Ley AC, Mauzerall DC: Absolute absorption cross-sections for Photosystem II and the minimum quantum requirement for photosynthesis in *Chlorella vulgaris,* Biochimica et Biophysica Acta (BBA) - Bioenergetics 680(1):95–106, 1982.

Li T, Zheng Y, Yu L, et al: Mixotrophic cultivation of a *Chlorella sorokiniana* strain for enhanced biomass and lipid production, Biomass and Bioenergy 66:204–213, 2014.

Malkin S, Fork DC: Bill Arnold and calorimetric measurements of the quantum requirement of photosynthesis? once again ahead of his time, Photosynthesis Research 48(1-2):41–46, 1996.

McCree KJ: The action spectrum, absorptance and quantum yield of photosynthesis in crop plants, Agricultural Meteorology 9(3):191–216, 1971.

Merzlyak M N, Razi Naqvi K: On recording the true absorption spectrum and the scattering spectrum of a turbid sample: application to cell suspensions of the cyanobacterium *Anabaena variabilis*, Journal of Photochemistry and Photobiology B: Biology, 58(2-3):123–129, 2000.

Meyer zu Tittingdorf JMW, Rexroth S, Schäfer E, et al: The stoichiometry of the chloroplast ATP synthase oligomer III in *Chlamydomonas reinhardtii* is not affected by the metabolic state, Biochimica et Biophysica Acta (BBA) - Bioenergetics, 1659(1):92–99, 2004.

Moberg AK, Ellem GK, Jameson GJ, et al: Simulated cell trajectories in a stratified gas–liquid flow tubular photobioreactor, Journal of Applied Phycology 24(3):357–363, 2011.

De Mooij T, Janssen M, Cerezo-chinarro O, et al: Antenna size reduction as a strategy to increase biomass productivity : a great potential not yet realized, Journal of Applied Phycology 27(3):1063-1077, 2014.

Müller P, Li XP, Niyogi KK: Non-photochemical quenching. A response to excess light energy, Plant Physiology 125(April):1558–1566, 2001.

Mullineaux CW: Co-existence of photosynthetic and respiratory activities in cyanobacterial thylakoid membranes, Biochimica et Biophysica Acta - Bioenergetics 1837(4):503–511, 2014.

Mullineaux CW, Emlyn-Jones D: State transitions: an example of acclimation to low-light stress, Journal of Experimental Botany 56(411):389–93, 2005.

Nixon PJ, Michoux F, Yu J, et al: Recent advances in understanding the assembly and repair of photosystem II, Annals of Botany 106(1):1–16, 2010.

Niyogi KK, Truong TB: Evolution of flexible non-photochemical quenching mechanisms that regulate light harvesting in oxygenic photosynthesis, Current Opinion in Plant Biology 16(3):307–14, 2013.

Nogales J, Gudmundsson S, Knight EM, et al: Detailing the optimality of photosynthesis in cyanobacteria through systems biology analysis, Proceedings of the National Academy of Sciences of the United States of America 109(7):2678–83, 2012.

Oldenhof H, Zachleder V, Van Den Ende H: Blue- and red-light regulation of the cell cycle in *Chlamydomonas reinhardtii* (Chlorophyta), European Journal of Phycology 41(3):313-320, 2006.

Olivieri G, Gargiulo L, Lettieri P, et al: Photobioreactors for microalgal cultures: A Lagrangian model coupling hydrodynamics and kinetics, Biotechnology Progress, published online 27 July 2015, doi: 10.1002/btpr.2138.

Perner-Nochta I, Posten C: Simulations of light intensity variation in photobioreactors, Journal of Biotechnology 131(3):276–85, 2007.

Phillips JN, Myers J: Growth Rate of *Chlorella* in Flashing Light, Plant Physiology 29(8):152–161, 1954.

Pirt SJ: The maintenance energy of bacteria in growing cultures, Proceedings of the Royal Society B: Biological Sciences 163(991):224–231, 1965.

Pogoryelov D, Reichen C, Klyszejko AL, et al: The oligomeric state of c rings from cyanobacterial F-ATP synthases varies from 13 to 15, Journal of Bacteriology 189(16):5895–902, 2007.

Qiang H, Richmond A: Productivity and photosynthetic efficiency of *Spirulina platensis* as affected by light intensity, algal density and rate of mixing in a flat plate photobioreactor, Journal of Applied Phycology 8(2):139–145, 1996.

Ross ON, Geider RJ: New cell-based model of photosynthesis and photo-acclimation: accumulation and mobilisation of energy reserves in phytoplankton, Marine Ecology Progress Series 383:53–71, 2009.

Rubio Camacho F, García Camacho F, Fernández Sevilla JM, et al: A mechanistic model of photosynthesis in microalgae, Biotechnology and Bioengineering 81(4):459–473, 2003.

Seelert H, Poetsch A, Dencher NA, et al: Proton-powered turbine of a plant motor, Nature 405(May):418–419, 2000.

Shi XM, Chen F, Yuan JP, et al: Heterotrophic production of lutein by selected *Chlorella* strains, Journal of Applied Phycology 9(5):445–450, 1997.

Stitt M: Limitation of photosynthesis by carbon metabolism : I. Evidence for excess electron transport capacity in leaves carrying out photosynthesis in saturating light and CO_2, Plant Physiology 81(4):1115–1122, 1986.

Sukenik A, Falkowski PG, Bennett J: Potential enhancement of photosynthetic energy conversion in algal mass culture, Biotechnology and Bioengineering 30:970–977, 1987.

Takache H, Pruvost J, Cornet JF: Kinetic modeling of the photosynthetic growth of *Chlamydomonas reinhardtii* in a photobioreactor, Biotechnology Progress 28(3):681–692, 2012.

Takache H, Pruvost J, Marec H, Investigation of light/dark cycles effects on the photosynthetic growth of *Chlamydomonas reinhardtii* in conditions representative of photobioreactor cultivation, Algal Research 8:192–204, 2015.

Tamburic B, Szabó M, Tran N-AT, et al: Action spectra of oxygen production and chlorophyll a fluorescence in the green microalga *Nannochloropsis oculata*, Bioresource Technology 169:320–327, 2014.

Tanada T: The Photosynthetic Efficiency of Carotenoid Pigments in *Navicula minima*, American Journal of Botany 38(4):276-283, 1951.

Ünlü C, Drop B, Croce R, et al: State transitions in *Chlamydomonas reinhardtii* strongly modulate the functional size of photosystem II but not of photosystem I, Proceedings of the National Academy of Sciences of the United States of America 111(9):3460–3465, 2014.

Vejrazka C, Janssen M, Benvenuti G, et al: Photosynthetic efficiency and oxygen evolution of *Chlamydomonas reinhardtii* under continuous and flashing light, Applied Microbiology and Biotechnology 97(4):1523–32, 2013.

Vejrazka C, Janssen M, Streefland M, et al: Photosynthetic efficiency of *Chlamydomonas reinhardtii* in flashing light, Biotechnology and Bioengineering 108(12):2905–2913, 2011.

Vejrazka C, Streefland M, Wijffels RH, et al: The role of an electron pool in algal photosynthesis during sub-second light–dark cycling, Algal Research 12:43–51, 2015.

Vermaas WFJ: Photosynthesis and Respiration in Cyanobacteria, Encyclopedia of Life Sciences 161:1-7, 2001.

Vítová M, Bišová K, Kawano S, et al: Accumulation of energy reserves in algae: From cell cycles to biotechnological applications, Biotechnology Advances, published online 16 May 2015, doi:10.1016/j.biotechadv.2015.04.012

Vollmar M, Schlieper D, Winn M, et al: Structure of the c14 rotor ring of the proton translocating chloroplast ATP synthase, Journal of Biological Chemistry 284(27):18228–18235, 2009.

Von Stockar U, Liu J-S: Does microbial life always feed on negative entropy? Thermodynamic analysis of microbial growth, Biochimica et Biophysica Acta (BBA) - Bioenergetics 1412(3):191–211, 1999.

Wobbe L, Remacle C: Improving the sunlight-to-biomass conversion efficiency in microalgal biofactories, Journal of Biotechnology 201:28-42, 2014.

Zhang QH, Wu X, Xue SZ, et al: Hydrodynamic characteristics and microalgae cultivation in a novel flat-plate photobioreactor, Biotechnology Progress 29(1):127–34, 2012.

Zijffers J-W F, Schippers KJ, Zheng K, et al: Maximum photosynthetic yield of green microalgae in photobioreactors, Marine Biotechnology 12(6), 708–718, 2010.